# Some theoretical and numerical results for delayed neural field equations

Grégory Faye[1] and Olivier Faugeras[1]

[1]NeuroMathComp Laboratory, INRIA, Sophia Antipolis, CNRS, ENS Paris, France

December 24, 2009

**Abstract**

In this paper we study neural field models with delays which define a useful framework for modeling macroscopic parts of the cortex involving several populations of neurons. Nonlinear delayed integro-differential equations describe the spatio-temporal behavior of these fields. Using methods from the theory of delay differential equations, we show the existence and uniqueness of a solution of these equations. A Lyapunov analysis gives us sufficient conditions for the solutions to be asymptotically stable. We also present a fairly detailed study of the numerical computation of these solutions. This is, to our knowledge, the first time that a serious analysis of the problem of the existence and uniqueness of a solution of these equations has been performed. Another original contribution of ours is the definition of a Lyapunov functional and the result of stability it implies. We illustrate our numerical schemes on a variety of examples that are relevant to modeling in neuroscience.

**Keywords:** Neural fields; nonlinear integro-differential equations; delays; Lyapunov functional; pattern formation; numerical schemes.

## 1 Introduction

Delays arise naturally when we model neurobiological systems. For example, the finite-velocity propagation of action potentials, or the dendritic and synaptic processing can generate delays on the order of milliseconds. Effective delays can also be induced by the spike-generation dynamics. First, the delay due to propagation of action potentials along the axon depends on the travelled distance as well as on the type of neurons. Indeed, conduction velocities in the axon can range from about $1m.s^{-1}$ along unmyelinated axons to more than $100m.s^{-1}$ along myelinated ones [10, 20]. This is one of the reasons why significant time delays can emerge in certain brain structures. Second, some cells may have synapses or gap junctions on dendrites far from the cell body. In this case, there can also be a delay associated with the propagation of the action potential along the dendrite. Another delay can occur at a synaptic contact point in the transduction of an electrical signal into a biochemical signal and back again to a post-synaptic potential. Hence, the growing interest in understanding network models with space-dependent delays [2, 3, 8, 9, 14, 15, 16, 17, 18, 22].

In this paper, we focus on space-dependent delays. In particular we incorporate delays in the well-known Wilson and Cowan [23, 24] and Amari [1] models for neural fields. In order to cover both axonal and dendritic delays and contrary to most of the papers on the subject, we deal with very general delay integro-differential equations without specifying the form of the delays.

We present a general mathematical framework for the modeling of neural fields which is based on tools of delay-differential equation analysis and an original presentation and analysis of numerical schemes. We illustrate our results with numerical experiments. In section 2 we briefly introduce the equations, in section 3 we analyse the problem of the existence and uniqueness of their solutions. In section 4 we study the problem of their asymptotic stability. In the penultimate section, we present some numerical schemes for the actual computation of the solutions. Each numerical scheme is illustrated by numerical experiments. We conclude in section 6.

## 2 The models

Neural field models first appeared in the 50's, but the theory really took off in the 70's with the works of Wilson and Cowan [23, 24] and Amari [1]. Neural fields are continuous networks of interacting neural masses, describing the dynamics of the cortical tissue at the population level. These neural field models of population firing rate activity can be described, when delays are not taken into account by the following integro-differential equations:

$$\partial_t \mathbf{V}(r,t) = -L\mathbf{V}(r,t) + \int_\Omega \mathbf{W}(r,r',t)\mathbf{S}(\mathbf{V}(r',t))dr' + I_{\text{ext}}(r,t) \tag{1}$$

Let us briefly describe the various elements that appear in this equation before extending it to the case of delays.

We consider $n$ interacting populations of neurons whose state is described by their membrane potential $\mathbf{V}$, a vector of dimension $n$. The function $\mathbf{S} : \mathbb{R}^n \to \mathbb{R}^n$ is defined by $\mathbf{S}(x) = [S_1(x_1), \dots, S_n(x_n)]^T$ where $S_i$ is sigmoidal. The functions $S_i$ satisfy the properties introduced in the following definition:

**Definition 2.0.1.** *For all $i = 1, \dots, n$ $S_i$ and $S_i'$ are positive and bounded ($S_i'$ is the derivative of the function $S_i$). We note $S_{im}' = \sup_x S_i'(x)$, $S_m = \max_i \sup_x S_i(x)$ and $DS_m = \max_i S_{im}'$. Finally we define $D\mathbf{S}$ as the diagonal matrix* $\text{diag}(S_i')$.

The relation between the firing rate $\nu_i$ of population $i$ and its membrane potential $V_i$ is given by the relation $\nu_i = S_i(V_i)$.

The neuronal populations are distributed over some continuum, a bounded open subset $\Omega$ of $\mathbb{R}^q$, $q = 1, 2, 3$. The variables $r$ and $r'$ in (1) belong to $\Omega$. The $n \times n$ matrix $L$ is assumed to be diagonal, $L = \text{diag}(l_1, \cdots, l_n)$, where the positive number $l_i$ characterize the dynamics of the $i$th population, $i = 1, \cdots, n$. The $n \times n$ matrix function $\mathbf{W}(r,r',t)$ describes how the populations at point $r'$ influence those at point $r$ at time $t$. More precisely, $W_{i,j}(r,r',t)$ describes how population $j$ at point $r'$ influences population $i$ at point $r$ at time $t$. Finally $I_{\text{ext}}(r,t)$ is an external current that models external sources of excitation.

It is now straightforward to extend (1) to take into account space dependent delays. We introduce the $n$-dimensional vector function $\mathbf{d}(r,r')$ and assume its components to be non negative. $d_i(r,r')$ is the time it takes for the information about the $i$th population at location $r'$ to reach the populations at location $r$. Having said this we rewrite (1) as follows

$$\partial_t \mathbf{V}(r,t) = -L\mathbf{V}(r,t) + \int_\Omega \mathbf{W}(r,r',t)\mathbf{S}(\mathbf{V}(r',t-\mathbf{d}(r,r')))dr' + I_{\text{ext}}(r,t) \tag{2}$$

Equation (2) deals with vector quantities. We can also write the corresponding equation for each coordinate $i$ in $[\![1,n]\!]$:

$$\partial_t V_i(r,t) = -l_i V_i(r,t) + \sum_{j=1}^{n} \int_\Omega W_{i,j}(r,r,t)S_j(V_j(r',t-d_j(r,r')))dr' + I_{\text{ext}}^i(r,t)$$

## 3 Existence and uniqueness of a solution

In this section we deal with the problem of the existence and uniqueness of a solution to (2) for a given initial condition. We first introduce the framework in which this equation makes sense.

We start with the assumption that the state vector $\mathbf{V}$ is a differentiable (resp., square integrable) function of the time (resp. the space) variable. Let $\Omega$ be an open subset of $\mathbb{R}^q$ where $q = 1, 2, 3$ and $\mathcal{F}$ be the set $L^2(\Omega, \mathbb{R}^n)$ of the square integrable functions from $\Omega$ to $\mathbb{R}^n$. The Fischer-Riesz's theorem ensures that $\mathcal{F}$ is a Banach space for the norm: $\|\psi\|_{\mathcal{F}} = \sqrt{\sum_{i=1}^n \int_\Omega \psi_i^2(r)dr}$ for all $\psi \in \mathcal{F}$. We denote by $\mathcal{I}$ an interval of $\mathbb{R}$ containing 0.

### 3.1 The well-posedness of (2)

We define the Banach space $\mathcal{C} = \mathcal{C}([-d,0],\mathcal{F})$ of the continuous functions from $[-d,0]$ to $\mathcal{F}$ where $d = \sup_{\overline{\Omega}\times\overline{\Omega}} \mathbf{d}$ with the norm: $\|\phi\|_{\mathcal{C}} \overset{def}{=} \sup_{t\in[-d,0]} \|\phi(t)\|_{\mathcal{F}} = \sup_{t\in[-d,0]} \sqrt{\sum_{i=1}^{n} \int_\Omega \phi_i^2(r,t)dr}$. We need to introduce the following norms:

$$\forall W \in L^2(\Omega^2, \mathcal{M}_n(\mathbb{R})) \quad \|W\|_F = \sqrt{\sum_{i,j=1}^{n} \int_{\Omega^2} W_{ij}^2(r,r')drdr'}$$

$$\forall W \in \mathcal{C}(\mathcal{I}, L^2(\Omega^2, \mathcal{M}_n(\mathbb{R}))) \quad \|W\|_{\infty,F} = \sup_{t\in\mathcal{I}} \|W(t)\|_F$$

We use the traditional notation introduced by Hale in [12]:

$$\mathbf{X}_t(\theta) = \mathbf{X}(t+\theta) \quad \theta \in [-d,0]$$

when $\mathbf{X}_t \in \mathcal{C}$ for all $t \geq 0$. Equation (2) is formally recast as a retarded functional differential equation on the Banach space $\mathcal{F}$ with initial value $\phi \in \mathcal{C}$:

$$\begin{cases} \dot{\mathbf{V}}(t) = f(t, \mathbf{V}_t) \\ \mathbf{V}_0 = \phi \end{cases} \tag{3}$$

where $\mathbf{V}(t)$ is thought of as a mapping $\mathbf{V} : \mathcal{I} \to \mathcal{F}$. This means that $\mathbf{V}(t)$ is a function defined in $\Omega$ by $\mathbf{V}(t)(r) = \mathbf{V}(r,t)$, similarly we have $\mathbf{V}_t(\theta)(r) = \mathbf{V}(r,t+\theta)$. The function $f$ from $\mathcal{I}\times\mathcal{C}$ is equal to the righthand side of (2):

$$f(t,\mathbf{V}_t)(r) = -L\mathbf{V}_t(r,0) + \int_\Omega \mathbf{W}(r,r',t)\mathbf{S}(\mathbf{V}_t(r',-\mathbf{d}(r,r')))dr' + I_{\text{ext}}(r,t) \quad \forall t \geq 0 \quad \forall r \in \Omega$$

this means that $\forall \psi \in \mathcal{C}$:

$$f(t,\psi)(r) = -L\psi(r,0) + \int_\Omega \mathbf{W}(r,r',t)\mathbf{S}(\psi(r',-\mathbf{d}(r,r')))dr' + I_{\text{ext}}(r,t) \quad \forall r \in \Omega$$

We define by $\bar{\Omega}$ the closure of $\Omega$.

**Lemma 3.1.1.** *If the following assumptions are satisfied:*

- $W \in \mathcal{C}(\mathbb{R}, L^2(\Omega^2, \mathcal{M}_n(\mathbb{R})))$,
- $\mathbf{d} \in \mathcal{C}(\bar{\Omega}^2, \mathbb{R}_+^n)$,
- *the external current* $I_{ext} \in \mathcal{C}(\mathcal{I}, \mathcal{F})$,

*then $f$ is well defined and is from $\mathcal{I}\times\mathcal{C}$ to $\mathcal{F}$.*

*Proof.*

Since we work in an open bounded set $\Omega$, if $\phi \in \mathcal{C}$ then $S(\phi) \in \mathcal{F}$.

- Let $t \in \mathcal{I}$ and $\psi \in \mathcal{C}$. We introduce the mapping:

$$F : (t,\psi) \to F(t,\psi) \text{ such that } F(t,\psi)(r) = \int_\Omega \mathbf{W}(r,r',t)\psi(r',-\mathbf{d}(r,r'))dr'$$

We prove that $F(t,\psi)$ belongs to $\mathcal{F}$. We look at the i-th component:

$$\big(F(t,\psi)(r)\big)_i \leq \sum_{j=1}^{n} \left[\int_\Omega W_{i,j}^2(r,r',t)dr'\right]^{1/2} \left[\int_\Omega \psi_j^2(r',-d_j(r,r'))dr'\right]^{1/2}$$

$$\leq \sum_{j=1}^{n} \left[ \int_{\Omega} W_{i,j}^2(r,r',t)dr' \right]^{1/2} \sup_{s\in[-d,0]} \left[ \int_{\Omega} \psi_j^2(r',s)dr' \right]^{1/2}$$

$$\leq \left[ \sum_{j=1}^{n} \int_{\Omega} W_{i,j}^2(r,r',t)dr' \right]^{1/2} \left[ \sum_{j=1}^{n} \sup_{s\in[-d,0]} \|\psi_j(s)\|_2^2 \right]^{1/2}$$

$$= \|\psi\|_{\mathcal{C}} \left[ \sum_{j=1}^{n} \int_{\Omega} W_{i,j}^2(r,r',t)dr' \right]^{1/2}$$

So:

$$\|F(t,\psi)\|_{\mathcal{F}}^2 = \sum_{i=1}^{n} \int_{\Omega} \left( \sum_{j=1}^{n} \int_{\Omega} W_{i,j}(r,r',t)\psi_j(r',-d_j(r,r'))dr' \right)^2 dr$$

$$\leq \sum_{i=1}^{n} \int_{\Omega} \|\psi\|_{\mathcal{C}}^2 \sum_{j=1}^{n} \int_{\Omega} W_{i,j}^2(r,r',t)dr'dr \leq \|\psi\|_{\mathcal{C}}^2 \|\mathbf{W}(t)\|_F^2$$

- Then it is easy to see that $f(t,\psi)$ is well-defined and belongs to $\mathcal{F}$.

□

## 3.2 Existence and uniqueness of a solution

In this section we will deal with the problem of the existence and uniqueness of a solution to (3). Let $\mathcal{I} = [0,+\infty[$. Let us show existence and uniqueness on $[-d,+\infty[$.

**Theorem 3.2.1.** *If the following hypotheses are satisfied:*
*- $W \in \mathcal{C}(\mathcal{I}, L^2(\Omega^2, \mathcal{M}_n(\mathbb{R})))$,*
*- the external current $I_{ext} \in \mathcal{C}(\mathcal{I},\mathcal{F})$,*
*- $\mathbf{d} \in \mathcal{C}(\overline{\Omega}^2, \mathbb{R}_+^n)$,*
*Then for any $\phi \in \mathcal{C}$, there exists a unique solution $\mathbf{V} \in \mathcal{C}^1([0,+\infty[,\mathcal{F}) \cap \mathcal{C}([-d,+\infty[,\mathcal{F})$.*

*Proof.* Let $T > 0$ and show the existence and uniqueness on $[-d,T]$.
We have already proved that $f$ from $\mathcal{I}\times\mathcal{C}$ to $\mathcal{F}$ is well defined.
Let us prove that $f$ is continuous with respect to $(t,\psi)$:

$$f(t,\psi_1)(r) - f(s,\psi_2)(r) = -L(\psi_1(r,0) - \psi_2(r,0)) + \int_{\Omega} (\mathbf{W}(r,r',t) - \mathbf{W}(r,r',s))\mathbf{S}(\psi_1(r',-\mathbf{d}(r,r')))dr'$$

$$+ \int_{\Omega} \mathbf{W}(r,r',s)(\mathbf{S}(\psi_1(r',-\mathbf{d}(r,r'))) - \mathbf{S}(\psi_2(r',-\mathbf{d}(r,r'))))dr' + I_{ext}(r,t) - I_{ext}(r,s)$$

It follows that:

$$\|f(t,\psi_1) - f(s,\psi_2)\|_{\mathcal{F}} \leq l_m\|\psi_1-\psi_2\|_{\mathcal{C}} + \sqrt{n|\Omega|}S_m\|\mathbf{W}(.,.,t) - \mathbf{W}(.,.,s)\|_F$$

$$+DS_m\|W(.,.,s)\|_F\|\psi_1-\psi_2\|_{\mathcal{C}} + \|I_{ext}(.,t) - I_{ext}(.,s)\|_{\mathcal{F}}$$

Where $l_m = \max_{i=1,\dots,n}(l_i)$.
Because of the hypotheses on the continuity we can choose $|t-s|$ small enough so that $\|\mathbf{W}(.,.,t) - \mathbf{W}(.,.,s)\|_F$ and $\|I_{ext}(.,t) - I_{ext}(.,s)\|_{\mathcal{F}}$ are arbitrarily small. Since $W$ is continuous it is bounded in the neighborhood of $s$. This proves the continuity of $f$.
From the previous inequality we have:

$$\|f(t,\psi_1) - f(t,\psi_2)\|_{\mathcal{F}} \leq l_m\|\psi_1-\psi_2\|_{\mathcal{C}} + DS_m\|W(.,.,t)\|_F\|\psi_1-\psi_2\|_{\mathcal{C}}$$

This proves the Lipschitz continuity of $f$ with respect to its second argument. We apply theorem 2.3 of Hale [12], and conclude that there is a unique continuous function $\mathbf{V}$ defined on $[-d,T]$ that satisfies (3).

So this solution $\mathbf{V} \in \mathcal{C}([-d,T],\mathcal{F})$ and lemma 2.1 p.40 of Hale [12] ensures that $t \mapsto \mathbf{V}_t \in \mathcal{C}([0,T],\mathcal{C})$. However, we have proved that $f \in \mathcal{C}(\mathcal{I}\times\mathcal{C},\mathcal{F})$. It is then easy to see that $t \mapsto f(t,\mathbf{V}_t)$ is in $\mathcal{C}([0,T],\mathcal{F})$. This implies that $\dot{\mathbf{V}} \in \mathcal{C}([0,T],\mathcal{F})$ and so $\mathbf{V} \in \mathcal{C}^1([0,T],\mathcal{F})$. We obtain that $\forall T > 0$ there exists a solution on $[-d,T]$ satisfying $\mathbf{V} \in \mathcal{C}^1([0,T],\mathcal{F}) \cap \mathcal{C}([-d,T],\mathcal{F})$. If the maximum interval of existence is upper bounded, we can apply the previous analysis near this bound and extend the interval of existence, which is a contradiction. Finally the maximum interval of existence is $[-d,\infty[$.

□

### 3.3 Some remarks about the case $\Omega = \mathbb{R}^q$

Some very interesting work has been done on equation (2) in the case of a one-dimensional infinite continuum, $\Omega = \mathbb{R}$, and more rarely in the case of a two-dimensional infinite continuum, $\Omega = \mathbb{R}^2$. The reader is referred to the review papers by Venkov [22] and by Hutt and Atay [2] as well as to [15, 14, 9, 3]. Aside from the fact that an infinite cortex is unrealistic, the case $\Omega = \mathbb{R}^q$ raises some interesting mathematical questions. Indeed, we no longer have finite delays, so we cannot use the previous theorems. The work of Wu [25] provides the beginning of an answer.

## 4 Linear stability analysis in the autonomous case

The goal of this section is to work at a fixed point $\mathbf{V}^0$ of (2) and study a linear retarded functional differential equation. The theory introduced by Hale in [12] is based on autonomous systems, this is why we need to impose that the connectivity does not depend on the time $t$, we note $\mathbf{W}(r,r')$. For the moment, we impose that $\mathbf{W} \in L^2(\Omega^2,\mathcal{M}_n(\mathbb{R}))$. This section is divided into three parts. First we perform the linearization of (2) at a fixed point, then we study the stability by the method of Lyapunov functional, and finally we explain and compare our study to previous work.

### 4.1 The linearization

Let $\mathbf{V}^0$ be a fixed point of (2), *i.e.* $\mathbf{V}^0$ satisfies:

$$0 = -L\mathbf{V}^0(r) + \int_\Omega \mathbf{W}(r,r')\mathbf{S}(\mathbf{V}^0(r'))dr' + I_{\text{ext}}(r) \quad \forall r \in \Omega$$

We define a new connectivity:

$$\forall (r,r') \in \Omega^2 \quad \widetilde{\mathbf{W}}(r,r') = \mathbf{W}(r,r') \cdot D\mathbf{S}(\mathbf{V}^0(r'))$$

**Proposition 4.1.1.** *Let $\Omega$ be an open set and $\boldsymbol{W} \in L^2(\Omega^2,\mathcal{M}_n(\mathbb{R}))$ then $\widetilde{\boldsymbol{W}} \in L^2(\Omega^2,\mathcal{M}_n(\mathbb{R}))$.*

*Proof.*

$$\forall 1 \le i,j \le n \quad \left(\widetilde{\mathbf{W}}(r,r')\right)_{i,j} = \widetilde{W}_{i,j}(r,r') = \sum_{k=1}^{n} W_{i,k}(r,r')D\mathbf{S}(\mathbf{V}^0(r'))_{k,j}$$

then

$$\forall 1 \le i,j \le n \quad \widetilde{W}_{i,j}(r,r')^2 \le n\sum_{k=1}^{n} W_{i,k}(r,r')^2\left(D\mathbf{S}(\mathbf{V}^0(r'))_{k,j}\right)^2 \le nDS_m^2\sum_{k=1}^{n} W_{i,k}(r,r')^2$$

And we have the following inequalities:

$$\int_{\Omega^2} \widetilde{W}_{i,j}(r,r')^2 drdr' \le nDS_m^2 \int_{\Omega^2} W_{i,j}(r,r')^2 drdr' < \infty \quad \text{because} \quad \mathbf{W} \in L^2(\Omega^2,\mathcal{M}_N(\mathbb{R})).$$

We can conclude, thanks to Fubini's theorem, that $\widetilde{\mathbf{W}} \in L^2(\Omega^2,\mathcal{M}_n(\mathbb{R}))$. □

We are now able to define on $\mathcal{F}$ the linearized equation around $\mathbf{V}^0$:

$$\partial_t \mathbf{U}(r,t) = -L\mathbf{U}(r,t) + \int_\Omega \widetilde{\mathbf{W}}(r,r')\mathbf{U}(r',t-\mathbf{d}(r,r'))dr' \quad \forall t \geq 0 \quad \forall r \in \Omega \tag{4}$$

If 0 is asymptotically stable for (4) then $\mathbf{V}^0$ is also asymptotically stable for (2). This result, already known in finite dimensions, is non trivial to establish in infinite dimensions because it requires the study of the characteristic values of the infinitesimal generator associated to (4).

## 4.2 Stability by the method of Lyapunov functionals

### 4.2.1 Theoretical results

In this part we generalize an article published by Hale in 1963 [11] by extending his results to equations defined in an infinite dimensional space.
Let $\mathcal{C} = \mathcal{C}([-d,0],\mathcal{F})$ be the space of continuous functions taking the interval $[-d,0]$ into the Banach space $\mathcal{F}$. If $x$ is any continuous function defined on $[-d,T[$, $T>0$, then $x_t$ will denote an element of $\mathcal{C}$ for each $t \in [0,T[$ defined by $x_t(\theta) = x(t+\theta)$, $-d \leq \theta \leq 0$. If $f$ is any function mapping $\mathcal{C}$ into $\mathcal{F}$, we can define the following functional-differential equation:

$$\begin{cases} \frac{dx}{dt}(t) = f(x_t) \quad t \geq 0 \\ x_0 = \phi \end{cases} \tag{5}$$

**Hypothesis 4.2.1.** *In the following, we assume that $\mathcal{H} = \{\phi \in \mathcal{C} : \|\phi\| < H\}$ where $H > 0$, $f(0) = 0$ and $f$ is locally Lipschitz in $\mathcal{H}$.*

**Lemma 4.2.1.** *If $x(\phi)$ is a solution of (5) with initial function $\phi$ at 0, defined on $[-d,\infty[$ and $\|x_t(\phi)\| \leq H_1 < H$ for all $t \geq 0$, then the family of functions $\{x_t(\phi), t \geq 0\}$ belongs to a compact set of $\mathcal{C}$.*

*Proof.* As $f$ is locally Lipschitz in $\mathcal{H}$, for any $H_1 < H$ there exists a constant $L$ such that $\|f(\phi)\| \leq L$ for all $\phi$ with $\|\phi\| \leq H_1$. Moreover, for all $t \geq 0$, $x_t(\phi) \in \mathcal{C}$ *i.e* $x_t(\phi)(\theta) = x(\phi)(t+\theta)$ for all $\theta \in [-d,0]$.
If $\|x_t(\phi)\| \leq H_1 < H$ for all $t \geq 0$, then $\dot{x}(t) = f(x_t) \leq L$ and so $\|x(\phi)(t)\| \leq \|x(\phi)(0)\| + tL$ with $0 \leq t$.
But, $x(\phi)$ is a continuous function on $[-d,\infty[$ and $\|x(\phi)(t)\| \leq at + b$ for all $t \geq 0$ and $a > 0, b \geq 0$ so $x(\phi)$ is uniformly continuous on $[-d,\infty[$.
Consequently, $\{x_t(\phi), t \geq 0\}$ is uniformly equicontinuous. Arzela-Ascoli's theorem gives the conclusion. □

**Definition 4.2.1.** *An element $\psi$ of $\mathcal{C}$ is in $\omega(\phi)$, the $\omega$-limit set of $\phi$, if $x(\phi)$ is defined on $[-d,\infty[$ and there is a sequence of nonnegative real numbers $t_n \to \infty$ as $n \to \infty$ such that $\|x_{t_n}(\phi) - \psi\| \to 0$ as $n \to \infty$.*

**Lemma 4.2.2.** *If $\phi \in \mathcal{C}$ is such that the solution of (5) with initial function $\phi$ at 0 is defined on $[-d,\infty[$ and $\|x_t(\phi)\| \leq H_1 < H$ for all $t \geq 0$, then $\omega(\phi)$ is a nonempty, compact, invariant set and $dist(x_t(\phi),\omega(\phi)) \to 0$ as $t \to \infty$.*

*Proof.* Let be $t_n$ a sequence of nonnegative real numbers such as $t_n \to \infty$ as $n \to \infty$. The sequence $\left(x_{t_n}(\phi)\right)_n$ is included in a compact set of $\mathcal{C}$ thanks to lemma 4.2.1, so there exists a convergent subsequence and its limit is by definition in $\omega(\phi)$ which is nonempty.
Let now $\psi_n$ be a convergent sequence of $\omega(\phi)$ with $\psi = \lim_{t_n \to \infty} \psi_n$. For each $n$ there exists a sequence $t_m^n$ such that $x_{t_m^n}(\phi) \to \psi_n$ as $m \to \infty$. We choose $m(n)$ in order to have $t_n \overset{\text{def}}{=} t_{m(n)}^n > n$ and $\|x_{t_n}(\phi) - \psi_n\| < \frac{1}{n}$. So we have $\|x_{t_n}(\phi) - \psi\| \to 0$ as $n \to \infty$ and $\psi \in \omega(\phi)$. Thus $\omega(\phi)$ is closed and since, according to lemma 4.2.1, it is included in a compact set, it is compact. The proof also shows that $dist(x_t(\phi),\omega(\phi)) \to 0$ as $t \to \infty$ and it is easy to verify that $\omega(\phi)$ is an invariant set. □

**Definition 4.2.2.** *If $\mathcal{V}$ is a continuous scalar function defined on $\mathcal{H}$, we denote by $\dot{\mathcal{V}}$ its derivative along the solutions of (5) which is defined as:*

$$\dot{\mathcal{V}}(x_t(\phi)) = \limsup_{h \to 0^+} \frac{1}{h}\big(\mathcal{V}(x_{t+h}(\phi)) - \mathcal{V}(x_t(\phi))\big)$$

*We say that $\mathcal{V} : \mathcal{C} \to \mathbb{R}^+$ is a Lyapunov functional on a set $\mathcal{G} \in \mathcal{C}$ relative to (5) if $\mathcal{V}$ is continuous on $\bar{\mathcal{G}}$ (the closure of $\mathcal{G}$) and $\dot{\mathcal{V}} \leq 0$ on $\mathcal{G}$.*
*Let $\mathcal{M}$ be the largest set in $\{\phi \in \bar{\mathcal{G}} : \dot{\mathcal{V}}(\phi) = 0\}$ which is invariant with respect to (5).*

**Theorem 4.2.1.** *If $\mathcal{V}$ is a Lyapunov function on $\mathcal{U}_l = \{\phi \in \mathcal{C} : \mathcal{V}(\phi) < l\}$ and there is a constant $K$ such that $\phi \in \mathcal{U}_l$ implies $\|\phi(0)\| < K$, then any solution $x_t(\phi)$ of (5) with $\phi \in \mathcal{U}_l$ satisfies $x_t(\phi) \to \mathcal{M}$ as $t \to \infty$.*

*Proof.* If $\phi \in \mathcal{U}_l$ and $\dot{\mathcal{V}} \leq 0$ on $\mathcal{U}_l$, then $x_t(\phi) \in \mathcal{U}_l$ and $\|x(\phi)(t)\| \leq K$ for $t \geq 0$ which implies that $x_t(\phi)$ is bounded. By the lemma 4.2.2 $\omega(\phi)$ is an invariant, nonempty compact set. Since $\mathcal{V}(x_t(\phi))$ is nonincreasing and bounded below, $\mathcal{V}(x_t(\phi))$ has a limit $l_0 < l$ as $t \to \infty$. Since $\mathcal{V}$ is continuous on $\bar{\mathcal{U}}_l$, $\mathcal{V}(\psi) = l_0$ for $\psi \in \omega(\phi)$, or $\psi \in \omega(\phi)$ is invariant so $\dot{\mathcal{V}}(\psi) = 0$. Consequently $\omega(\phi)$ is in $\mathcal{M}$ and lemma 4.2.2 implies that $x_t(\phi) \to \mathcal{M}$ as $t \to \infty$. □

**Theorem 4.2.2.** *Suppose that there exists a Lyapunov function $\mathcal{V}$ defined on $\mathcal{C}$ which satisfies the following conditions:*

1. *$u(\|\phi(0)\|_{\mathcal{F}}) \leq \mathcal{V}(\phi) \leq v(\|\phi\|_{\mathcal{C}})$ where $u$ and $v$ are continuous nondecreasing real functions, $u(s)$ and $v(s)$ are positive for $s > 0$, and $u(0) = v(0) = 0$.*
2. *$u(s) \to \infty$ as $t \to \infty$.*
3. *$\dot{\mathcal{V}}(\phi) \leq -w(\|\phi(0)\|_{\mathcal{F}})$ where $w$ is a continuous nondecreasing real function, positive for $s > 0$, and such that $w(0) = 0$.*

*Then the solution $x = 0$ of (5) is uniformly asymptotically stable and all solutions of (5) approach zero as $t \to \infty$.*

*Proof.* The fact that the solution $x = 0$ of (5) is uniformly asymptotically stable is proved in [12], theorem 2.1. For the second part, we apply theorem 4.2.1 with $\mathcal{M} = \{0\}$ since it is easy to verify that all the conditions of the theorem are satisfied. □

### 4.2.2 The Lyapunov functional

We now define a Lyapunov function for equation (4) and use these theoretical results in order to study the stability of the 0 solution.

**Rescaling the equation** In order to establish a stability bound, we rescale equation (4) by $\frac{t}{\lambda}$ where $\lambda$ is a parameter which will be chosen later. Equation (4) becomes:

$$\partial_t \mathbf{U}(r,t) = -\lambda L\mathbf{U}(r,t) + \lambda \int_\Omega \widetilde{\mathbf{W}}(r,r')\mathbf{U}(r', t - \frac{\mathbf{d}(r,r')}{\lambda})dr' \quad \forall t \geq 0 \tag{6}$$

We recall that the above equation means: $\forall i = 1, \ldots, n$ and $\forall t \geq 0$:

$$\partial_t U_i(r,t) = -\lambda l_i U_i(r,t) + \lambda \sum_{j=1}^{n} \int_\Omega \widetilde{W}_{i,j}(r,r')U_j(r', t - \frac{d_j(r,r')}{\lambda})dr'$$

**Definition of the Lyapunov functional** We now introduce the Lyapunov functional that will allow us to conclude on the stability of (6). We use the notation introduced in the previous section, $\mathbf{U}_t$ means that, for all $t \geq 0$ we have $\mathbf{U}_t(\theta) = \mathbf{U}(t + \theta)$ for all $\theta \in [-d, 0]$.

$$\mathcal{V}(\mathbf{U}_t) = \frac{1}{2}\sum_{i=1}^{n} \int_\Omega l_i^{-1} U_i(r,t)^2 dr + \int_\Omega \beta(r) \sum_{i=1}^{n} \int_\Omega \int_{-\frac{d_i(r,r')}{\lambda}}^{0} U_i(r', t+\theta)^2 d\theta dr' dr$$

where $\beta \in L^1(\Omega, \mathbb{R})$ is defined below in (8).

**Deriving the Lyapunov functional** We want to obtain the derivative of $\mathcal{V}$, and for this, we recall the following result:

**Lemma 4.2.3.**

$$\frac{d}{dt}\left(\int_{\frac{d(r,r')}{\lambda}}^{0} f(r',t+\theta)^2 d\theta\right) = f(r',t)^2 - f(r',t-\frac{d(r,r')}{\lambda})^2$$

*Proof.*

$$\int_{\frac{d(r,r')}{\lambda}}^{0} f(r',t+\theta)^2 d\theta = \int_{t-\frac{d(r,r')}{\lambda}}^{t} f(r',\theta)^2 d\theta$$

The lemma follows directly from this equality. □

We define the derivative of $\mathcal{V}$ by:

$$\dot{\mathcal{V}}(\mathbf{U}_t) = \frac{d}{dt}\mathcal{V}(\mathbf{U}_t)$$

Thanks to lemma 4.2.3 we have:

$$\begin{aligned}\dot{\mathcal{V}}(\mathbf{U}_t) = \sum_{i=1}^{n}\int_\Omega U_i(r,t)\partial_t U_i(r,t)dr + \int_\Omega \beta(r)\sum_{i=1}^{n}\int_\Omega \left(U_i(r',t)^2 - U_i(r',t-\frac{d_i(r,r')}{\lambda})^2\right)dr'dr = \\ -\lambda\sum_{i=1}^{n}\int_\Omega U_i(r,t)^2 dr + \lambda\sum_{i=1}^{n}\int_\Omega U_i(r,t)\sum_{j=1}^{n}\int_\Omega l_i^{-1}\widetilde{W}_{i,j}(r,r')U_j(r',t-\frac{d_j(r,r')}{\lambda})dr'dr + \\ \left(\int_\Omega \beta(r)dr\right)\sum_{i=1}^{n}\int_\Omega U_i(r,t)^2 dr - \int_\Omega \beta(r)\sum_{i=1}^{n}\int_\Omega U_i(r',t-\frac{d_i(r,r')}{\lambda})^2 dr'dr\end{aligned}$$

**The choice of $\beta$** We now have choose an acceptable $\beta$. We want to bound the derivative $\dot{\mathcal{V}}(\mathbf{U}_t)$ by a quadratic form in the variables $X = \sqrt{\sum_{i=1}^{n}\int_\Omega U_i(r,t)^2 dr}$ and $Y = \sqrt{\int_\Omega \beta(r)\left(\sum_{j=1}^{n}\int_\Omega U_j(r',t-\frac{d_j(r,r')}{\lambda})^2 dr'\right)dr}$.
We already know that:

$$\dot{\mathcal{V}}(\mathbf{U}_t) = \left(\int_\Omega \beta(r)dr - \lambda\right)X^2 + \lambda\sum_{i=1}^{n}\int_\Omega U_i(r,t)\sum_{j=1}^{n}\int_\Omega l_i^{-1}\widetilde{W}_{i,j}(r,r')U_j(r',t-\frac{d_j(r,r')}{\lambda})dr'dr - Y^2,$$

thus, it remains to bound

$$\Gamma(\mathbf{U}) = \sum_{i=1}^{n}\int_\Omega U_i(r,t)\sum_{j=1}^{n}\int_\Omega l_i^{-1}\widetilde{W}_{i,j}(r,r')U_j(r',t-\frac{d_j(r,r')}{\lambda})dr'dr \tag{7}$$

by a homogeneous polynomial of degree two in $X$ and $Y$.
Using the Cauchy-Schwarz inequality in $L^2(\mathbb{R})$ and $\mathbb{R}^n$, we get:

$$\begin{aligned}\sum_{j=1}^{n}\int_\Omega l_i^{-1}\widetilde{W}_{i,j}(r,r')U_j(r',t-\frac{d_j(r,r')}{\lambda})dr' \leq \\ \sum_{j=1}^{n}\sqrt{\int_\Omega l_i^{-2}\widetilde{W}_{i,j}(r,r')^2 dr'}\sqrt{\int_\Omega U_j(r',t-\frac{d_j(r,r')}{\lambda})^2 dr'} \leq \\ \sqrt{\sum_{j=1}^{n}\int_\Omega l_i^{-2}\widetilde{W}_{i,j}(r,r')^2 dr'}\sqrt{\sum_{j=1}^{n}\int_\Omega U_j(r',t-\frac{d_j(r,r')}{\lambda})^2 dr'}.\end{aligned}$$

We substitute this inequality in $\Gamma(\mathbf{U})$:

$$\Gamma(\mathbf{U}) \leq \sum_{i=1}^{n} \int_{\Omega} U_i(r,t) \sqrt{\sum_{j=1}^{n} \int_{\Omega} l_i^{-2} \widetilde{W}_{i,j}(r,r')^2 dr'} \sqrt{\sum_{j=1}^{n} \int_{\Omega} U_j(r', t - \frac{d_j(r,r')}{\lambda})^2 dr' dr}$$

Once again, by the Cauchy-Schwarz inequality in $L^2(\mathbb{R})$ and $\mathbb{R}^n$, we have:

$$\Gamma(\mathbf{U}) \leq \sum_{i=1}^{n} \sqrt{\int_{\Omega} U_i(r,t)^2 dr} \sqrt{\int_{\Omega} \Big( \sum_{j=1}^{n} \int_{\Omega} l_i^{-2} \widetilde{W}_{i,j}(r,r')^2 dr' \Big) \Big( \sum_{j=1}^{n} \int_{\Omega} U_j(r', t - \frac{d_j(r,r')}{\lambda})^2 dr' \Big) dr} \leq$$
$$\sqrt{\sum_{i=1}^{n} \int_{\Omega} U_i(r,t)^2 dr} \sqrt{\sum_{i=1}^{N} \int_{\Omega} \Big( \sum_{j=1}^{n} \int_{\Omega} l_i^{-2} \widetilde{W}_{i,j}(r,r')^2 dr' \Big) \Big( \sum_{j=1}^{n} \int_{\Omega} U_j(r', t - \frac{d_j(r,r')}{\lambda})^2 dr' \Big) dr} =$$
$$\sqrt{\sum_{i=1}^{n} \int_{\Omega} U_i(r,t)^2 dr} \sqrt{\int_{\Omega} \Big( \sum_{i,j=1}^{n} \int_{\Omega} l_i^{-2} \widetilde{W}_{i,j}(r,r')^2 dr' \Big) \Big( \sum_{j=1}^{n} \int_{\Omega} U_j(r', t - \frac{d_j(r,r')}{\lambda})^2 dr' \Big) dr}$$

This suggests the following choice:

$$\beta(r) = \sum_{i,j=1}^{n} \int_{\Omega} l_i^{-2} \widetilde{W}_{i,j}(r,r')^2 dr' \tag{8}$$

**The result** We have

$$\dot{\mathcal{V}}(\mathbf{U}_t) \leq \sum_{i=1}^{n} \int_{\Omega} \Big( \int_{\Omega} \beta(r) dr - \lambda \Big) U_i(r,t)^2 dr - \int_{\Omega} \beta(r) \sum_{i=1}^{n} \int_{\Omega} U_i(r', t - \frac{d_i(r,r')}{\lambda})^2 dr' dr +$$
$$\lambda \sqrt{\sum_{i=1}^{n} \int_{\Omega} U_i(r,t)^2 dr} \sqrt{\int_{\Omega} \beta(r) \Big( \sum_{j=1}^{n} \int_{\Omega} U_j(r', t - \frac{d_j(r,r')}{\lambda})^2 dr' \Big) dr}.$$

If we note

$$X = \sqrt{\sum_{i=1}^{n} \int_{\Omega} U_i(r,t)^2 dr} \quad Y = \sqrt{\int_{\Omega} \beta(r) \Big( \sum_{j=1}^{n} \int_{\Omega} U_j(r', t - \frac{d_j(r,r')}{\lambda})^2 dr' \Big) dr},$$

we have:

$$\dot{\mathcal{V}}(\mathbf{U}_t) \leq \Big( \int_{\Omega} \beta(r) dr - \lambda \Big) X^2 + \lambda XY - Y^2.$$

We recall that if $\mathbf{W} \in L^2(\Omega^2, \mathcal{M}_n(\mathbb{R}))$:

$$\|\mathbf{W}\|_F = \sqrt{\sum_{i,j=1}^{n} \int_{\Omega} \int_{\Omega} W_{i,j}(r,r')^2 dr' dr}$$

This leads us to the following proposition.

**Proposition 4.2.1.** *If* $\int_{\Omega} \beta(r) dr < \lambda - \frac{\lambda^2}{4}$ *then* $\dot{\mathcal{V}}(\mathbf{U}_t) < -\epsilon \sum_{i=1}^{n} \int_{\Omega} U_i(r,t)^2 dr$, *where* $\epsilon = \lambda - \frac{\lambda^2}{4} - \int_{\Omega} \beta(r) dr$.

*Proof.* As we have:

$$\dot{\mathcal{V}}(\mathbf{U}_t) \leq \big( \int_{\Omega} \beta(r) dr - \lambda \big) X^2 + \lambda XY - Y^2,$$

if $\int_\Omega \beta(r)dr < \lambda - \frac{\lambda^2}{4}$ then $\epsilon = \lambda - \frac{\lambda^2}{4} - \int_\Omega \beta(r)dr$ and:

$$\Big(\int_\Omega \beta(r)dr - \lambda\Big)X^2 + \lambda XY - Y^2 =$$
$$-(Y - \lambda\frac{X}{2})^2 + \frac{\lambda^2 X^2}{4} + \Big(\int_\Omega \beta(r)dr - \lambda\Big)X^2 =$$
$$-(Y - \frac{X}{2})^2 - \epsilon X^2 \leq -\epsilon X^2,$$

then $\dot{\mathcal{V}}(\mathbf{U}_t) \leq -\epsilon \int_\Omega \mathbf{U}(r,t)^2 dr$. □

We therefore choose for $\lambda$ the maximum of the function $\Lambda : x \mapsto x - \frac{x^2}{4}$ which is reached for $x = 2$ and is equal to $\Lambda(2) = 1$. We rewrite $\int_\Omega \beta(r)dr$ in the convenient form

$$\int_\Omega \beta(r)dr = \|L^{-\frac{1}{2}}\widetilde{\mathbf{W}}L^{-\frac{1}{2}}\|_F^2, \tag{9}$$

and state the following theorem.

**Theorem 4.2.3.** *If $\|L^{-\frac{1}{2}}\widetilde{\boldsymbol{W}}L^{-\frac{1}{2}}\|_F < 1$ then $\boldsymbol{V}^0$ is uniformly asymptotically stable.*

*Proof.* Let

$$\mathcal{V}(\phi) = \frac{1}{2}\sum_{i=1}^n \int_\Omega l_i^{-1}\phi_i(r,0)^2 dr + \int_\Omega \beta(r)\sum_{i=1}^n \int_\Omega \int_{-\frac{d_i(r,r')}{2}}^0 \phi_i(r',\theta)^2 d\theta dr' dr,$$

where

$$\beta(r) = \sum_{i,j=1}^n \int_\Omega l_i^{-2}\widetilde{W}_{i,j}(r,r')^2 dr'$$

The following conditions are satisfied:
• There exists $u, v$ that satisfy: $u(\|\phi(0)\|_{\mathcal{F}}) \leq \mathcal{V}(\phi) \leq v(\|\phi\|_{\mathcal{C}})$ where $u$ and $v$ are continuous nondecreasing real functions, $u(s)$ and $v(s)$ are positive for $s > 0$ and $u(0) = v(0) = 0$. Indeed $\frac{l_m^{-1}}{2}\|\phi(0)\|_{\mathcal{F}}^2 \leq \mathcal{V}(\phi) \leq (\frac{\ell^{-1}}{2} + d\ell^{-2}\|\widetilde{\mathbf{W}}\|_F^2)\|\phi\|_{\mathcal{C}}^2$ and hence $u(s) = \frac{l_m^{-1}}{2}s^2$ and $v(s) = (\frac{\ell^{-1}}{2} + d\ell^{-2}\|\widetilde{\mathbf{W}}\|_F^2)s^2$.
• Thanks to proposition 4.2.1 we have $\dot{\mathcal{V}}(\phi) \leq -w(\|\phi(0)\|_{\mathcal{F}})$ and $w(s) = \epsilon s^2$ so $w(s) > 0$ if $s > 0$, $w$ is a continuous nondecreasing function.
So we can apply theorem 4.2.2 for functional equations and 0 is asymptotically stable for equation (4) and so is $\mathbf{V}^0$ for (2). □

## 4.3 Discussion of the bound

We have presented a method which gives a bound for the asymptotic stability. To our knowledge, Wu in [25] was the first to establish a bound of stability for general retarded functional differential equations. In our notations his bound can be written $\|\widetilde{\mathbf{W}}\|_F < \ell e^{-\ell d}$ which has the advantage to take into account the delays but has also the disadvantage to be very conservative. Atay and Hutt in [2] find a bound in the case of a one population equation, with $\Omega = \mathbb{R}$. We can recover a similar bound in our framework by changing the form of $\beta$. Indeed, we can bound (7) by:

$$\sqrt{\sum_{i=1}^n \int_\Omega U_i(r,t)^2 dr}\sqrt{\int_\Omega \Big(\sum_{i,j=1}^n \int_\Omega \ell^{-2}\widetilde{W}_{i,j}(r,r')^2 dr'\Big)\Big(\sum_{j=1}^n \int_\Omega U_j(r', t - \frac{d_j(r,r')}{\lambda})^2 dr'\Big)dr},$$

and choose $\beta(r) = \sum_{i,j=1}^n \int_\Omega \ell^{-2}\widetilde{W}_{i,j}(r,r')^2 dr'$ and so if $\|\widetilde{\mathbf{W}}\|_F < \ell$ then $\mathbf{V}^0$ is asymptotically stable. This shows that this bound is better than the one obtained by Wu.
Finally we see that our bound $\|L^{-\frac{1}{2}}\widetilde{\mathbf{W}}L^{-\frac{1}{2}}\|_F < 1$ obtained by the method of Lyapunov functional is the less conservative.

# 5 Numerical schemes

The aim of this section is to numerically solve equation (2) for different $n$ and $q$. We remind the reader that $n$ is the number of populations of neurons and $q$ is the spatial dimension. This implies developing a numerical scheme that approaches the solution of our equation, and to prove that this scheme effectively converges to the solution.

To our knowledge, only in the paper of Hutt et al. [17] and in the thesis of N.A. Venkov [21], has a numerical scheme been explicitly developed, but without really dealing with such numerical analysis questions as convergence. Notice also that most papers [2, 15, 17, 22, 14] that dealt with neural field equations with space-dependent delays only studied an equation of the type of (2) for $n = q = 1$ and $\Omega = \mathbb{R}$. In this section, we present new results concerning the cases $n = 1, 2$ with $\Omega$ an open bounded set of $\mathbb{R}$, and $n = 2$ with $\Omega$ a square region of $\mathbb{R}^2$.

Several computer codes have been developed in the last decades for the numerical integration of functional differential equations, for an overview see [4]. **dde23**, written in **Matlab**, can efficiently solve delay differential equations with constant delays. The code was developed by L.F. Shampine and S. Thompson [19]. We decided to make it the center of our numerical investigation. The main motivation of this choice was that this solver can deal with delay equations with a large number of constant delays. This turns out to be a big advantage, as shown later. We have divided this section into three parts. The first is dedicated to the study of (2) in one space dimension *i.e.* $q = 1$, with only one population of neurons whereas in the second part we deal with the richer case of two populations. The third part covers the case of one population of neurons in two dimensions in space. In each part we develop and analyse a numerical scheme which we illustrate with numerical experiments.

## 5.1 One space dimension, one population of neurons

In order to illustrate the notions that we have developed, we take the example of equation (2) in the case $n = q = 1$, which is the most often studied case. Let us consider the scalar integro-differential equation:

$$\begin{cases} \partial_t v(x,t) = -\alpha v(x,t) + \int_\Omega W(x,y) S\big(v(y, t - \tilde{d}(x,y))\big) dy + I_{\text{ext}}(x,t) \quad t \geq 0 \\ v(x,t) = \phi(x,t) \quad t \in [-d, 0] \end{cases} \tag{10}$$

where $d = \sup_{\overline{\Omega}^2} \tilde{d}(x,y)$ and $\Omega = ]-l, l[$. Note that most authors choose $\tilde{d}(x,y) = \frac{|x-y|}{c}$ because of its biological relevance. The numerical scheme that we are about to present can be used with a more general functional form of the delay. It is only for the numerical experiments that we return to the more biologically plausible form.
We assume that the connectivity function satisfies:

$$\forall x, y \in \mathbb{R} \quad W(x,y) = w(|x-y|).$$

Such connectivity functions are called homogeneous, since they are translation invariant, and isotropic, since $w$ is only a function of $|x|$. This implies that populations near the edges of the domain $\Omega$ receive fewer connections than populations in the middle. This implies that spatially uniform activities are not transformed to spatially uniform outputs.

We make the hypothesis that the delay is also a function of $|x-y|$ and that $\tilde{d}(0) = 0$. We write $\tilde{d}(|x-y|)$ for $\tilde{d}(x,y)$.
Finally, we assume that (10) has a unique solution $v$ defined on $[-d, +\infty[$.

### 5.1.1 Discretization scheme

We discretize $\Omega$ in order to turn (10) into a finite number of equations. For this purpose we introduce $h = \frac{|\Omega|}{m}$, $m \in \mathbb{N}^* = \mathbb{N} \setminus \{0\}$,

$$\forall i \in [\![1, m+1]\!] \quad x_i = -l + (i-1)h,$$

and obtain the $m+1$ equations:

$$\frac{dv}{dt}(x_i,t) = -\alpha v(x_i,t) + \int_\Omega w(x_i - y) S\big(v(y, t - \tilde{d}(|x_i - y|))\big) dy + I_{\text{ext}}(x_i,t),$$

which define the discretization of (10):

$$\begin{cases} \frac{d\tilde{v}}{dt}(t) = -\alpha\tilde{v}(t) + \mathbf{w}\cdot S(\tilde{v})(t) + \tilde{I}_{\text{ext}}(t) = F(t,\tilde{v}(t),\tilde{v}_t) \quad t \geq 0 \\ \tilde{v}(t) = \tilde{\phi}(t) \quad t \in [-d,0]. \end{cases} \tag{11}$$

$\tilde{v}(t) \in \mathbb{R}^{m+1}$, $\tilde{v}(t)_i = v(x_i,t)$ and the same definition holds for $\tilde{I}_{\text{ext}}$ and $\tilde{\phi}$. Moreover,

$$\mathbf{w}\cdot S(\tilde{v})(t)_i = \int_\Omega w(x_i-y)S\big(v(y,t-\tilde{d}(|x_i-y|))\big)dy$$

If we want to obtain constant delays, we have to discretize the integral term. For this, we use the trapezoidal rule $\int_a^b f(x)dx \cong \frac{b-a}{2}\big(f(a)+f(b)\big)$. For all $i = 1,\dots,m+1$ we have:

$$\int_{-l}^{l} w(x_i-y)S\big(v(y,t-\tilde{d}(|x_i-y|))\big)dy = \sum_{k=1}^{m}\int_{x_k}^{x_{k+1}} w(x_i-y)S\big(v(y,t-\tilde{d}(|x_i-y|))\big)dy.$$

But by the trapezoidal rule:

$$\int_{x_k}^{x_{k+1}} w(x_i-y)S\big(v(y,t-\tilde{d}(|x_i-y|))\big)dy \cong \\ h\frac{w(x_i-x_k)S\big(v(x_k,t-\tilde{d}(|x_i-x_k|))\big) + w(x_i-x_{k+1})S\big(v(x_{k+1},t-\tilde{d}(|x_i-x_{k+1}|))\big)}{2},$$

which implies

$$\int_{-l}^{l} w(x_i-y)S\big(v(y,t-\tilde{d}(|x_i-y|))\big)dy \cong \\ \frac{h}{2}\Big(w(x_i-x_1)S\big(v(x_1,t-\tilde{d}(|x_i-x_1|))\big) + w(x_i-x_{m+1})S\big(v(x_{m+1},t-\tilde{d}(|x_i-x_{m+1}|))\big)\Big) \\ + h\sum_{k=2}^{m-1} w(x_i-x_k)S\big(v(x_k,t-\tilde{d}(|x_i-x_k|))\big)$$

For each $i = 1,\dots,m+1$ we have:

$$\frac{dv}{dt}(x_i,t) \cong -\alpha v(x_i,t) + I_{\text{ext}}(x_i,t) + \frac{h}{2}w(x_i-x_1)S\big(v(x_1,t-\tilde{d}(|x_i-x_1|))\big) \\ + \frac{h}{2}w(x_i-x_{m+1})S\big(v(x_{m+1},t-\tilde{d}(|x_i-x_{m+1}|))\big) + h\sum_{k=2}^{m-1} w(x_i-x_k)S\big(v(x_k,t-\tilde{d}(|x_i-x_k|))\big)$$

Using the fact that $x_i - x_k = (i-k)h$ we end up with the following numerical scheme, where $v_i(t)$ is an approximation of $v(x_i,t)$:

$$\forall i = 1\dots m+1 \quad \frac{dv_i}{dt}(t) = -\alpha v_i(t) + I^i_{\text{ext}}(t) + \frac{h}{2}w\big((i-1)h\big)S\big(v_1(t-\tilde{d}(|i-1|h))\big) \\ + \frac{h}{2}w\big((i-m-1)h\big)S\big(v_{m+1}(t-\tilde{d}(|i-m-1|h))\big) + h\sum_{k=2}^{m-1} w\big((i-k)h\big)S\big(v_k(t-\tilde{d}(|i-k|h))\big)$$

In order to rewrite the previous equation in vector form we define the three vectors

$$V(t) = \begin{pmatrix} v_1(t) \\ \vdots \\ v_{m+1}(t) \end{pmatrix} \quad \Phi(t) = \begin{pmatrix} \phi_1(t) \\ \vdots \\ \phi_{m+1}(t) \end{pmatrix} \quad I_{\text{ext}}(t) = \begin{pmatrix} I^1_{\text{ext}}(t) \\ \vdots \\ I^{m+1}_{\text{ext}}(t) \end{pmatrix},$$

and the following matrices of $\mathcal{M}_{m+1}(\mathbb{R})$ the space of the square matrices of size $m+1 \times m+1$:

**Definition 5.1.1.** *Let $E_u$ and $E_d$ be the following two matrices in $\mathcal{M}_{m+1}(\mathbb{R})$:*

$$E_u = \begin{pmatrix} 0 & 1 & 0 & \dots & 0 \\ \vdots & \ddots & \ddots & \ddots & \vdots \\ \vdots & (0) & \ddots & \ddots & 0 \\ \vdots & (0) & (0) & \ddots & 1 \\ 0 & \dots & \dots & \dots & 0 \end{pmatrix} \quad E_d = E_u^T$$

*We then define $\forall k = 1, \dots, m$*

$$E_k = E_0(E_u^k + E_d^k),$$

*with* $E_0 = \begin{pmatrix} \frac{1}{2} & 0 & \dots & \dots & 0 \\ 0 & 1 & \ddots & (0) & 0 \\ \vdots & \ddots & \ddots & \ddots & \vdots \\ \vdots & (0) & \ddots & 1 & 0 \\ 0 & \dots & \dots & 0 & \frac{1}{2} \end{pmatrix}$.

This leads to the following proposition:

**Proposition 5.1.1.** *The trapezoidal rule applied to (11) leads to the following numerical scheme:*

$$\begin{cases} \frac{dV}{dt}(t) = -\alpha V(t) + \sum_{k=0}^{m} hw(kh)E_k S(V(t - \tilde{d}(kh))) + I_{ext}(t) \stackrel{def}{=} f(t, V(t), V(t-\tau_1), \dots, V(t-\tau_m)) \\ V(t) = \Phi(t) \quad t \in [-d, 0] \end{cases} \tag{12}$$

*where $V(t)$ is an approximation of $\tilde{v}(t)$ and $\tau_i = \tilde{d}(ih)$*

We remind the reader that our initial goal was to compute the solutions of (2). At this step of our study, we can directly solve (12) with the function **dde23** which is based on a step-by-step method. Bellen and Zennaro have studied in detail numerical methods for delay differential equations and the interested reader can find in their remarkable book [4] a survey of the step-by-step method.

### 5.1.2 Remark

For our numerical experiments, as mentioned above, we use the specific function **dde23**. We observe that the fact of dealing with constant delays constrains the choice of the quadrature rule. Indeed, we cannot use adaptative methods to discretize the integral because we would no longer have constant delays in our schemes. We see that if we use the method of discretization presented above, the quadrature rule will impose the error of convergence of our scheme. For example, with the trapezoidal rule, we cannot do better than $O(h^2)$. If we use Simpson's rule, we can have $O(h^4)$ at best.

These estimates hold under the assumption that the solution is very smooth in time (which is not a problem), but also in space. Indeed, with the example of the trapezoidal rule if $f$ is $\mathcal{C}^2$ on an interval $[a, b]$ the error of the rule is $-\frac{(b-a)^3}{12m^2} f^{(2)}(\xi)$ for some $\xi \in [a, b]$, where $m$ is the number of subintervals used on the interval $[a, b]$. In our case we have to look at the second derivative of the functions $W_i : y \to w(x_i - y)S\big(v(y, t - \tilde{d}(y - x_i))\big)$ on $[x_i, x_{i+1}]$ for $i = 1, \cdots, m$. If we want to control the error, we have to impose that the solution is, at least, $\mathcal{C}^2$ in time and in space. The quadrature rule preconditions the error of discretization with the consequence that even if we use a very accurate scheme in time (it is the case with **dde23**), the error will remain of the same order as the quadrature.

### 5.1.3 Convergence

We now provide a brief sketch of the proof of the convergence of our numerical scheme.
We assume for simplicity that there is no external input. We fix $x \in \Omega$ and apply the trapezoidal rule to (10) with the same discretization as in the previous section.

We have:

$$\partial_t v(x,t) \cong Q^m(v_t) \stackrel{def}{=} -\alpha v(x,t) + \frac{h}{2} w(x-x_1) S\big(v(x_1, t-\tilde{d}(|x-x_1|))\big) + \frac{h}{2} w(x-x_{m+1}) S\big(v(x_{m+1}, t-\tilde{d}(|x-x_{m+1}|))\big) + h \sum_{k=2}^{m-1} w(x-x_k) S\big(v(x_k, t-\tilde{d}(|x-x_k|))\big),$$

with:

$$\lim_{m\to+\infty} Q^m(v_t) = -\alpha v(x,t) + \int_\Omega W(x,y) S\big(v(y, t-\tilde{d}(x,y))\big) dy \stackrel{def}{=} Q(v_t).$$

We define the functional space $\mathcal{Q} = \mathcal{C}([-d,0], \mathcal{C}^2(\Omega))$. Clearly $Q \in \mathcal{Q}$. Let $v$ be the unique solution defined on $[-d,T]$ of

$$\begin{cases} \frac{dv}{dt}(t) = Q(v_t) & t \geq 0 \\ v_0 = \phi \end{cases}$$

The proof of this assumption can be directly adapted from the proof on the existence and the uniqueness of section 3. Then we can apply the theorem on the continuous dependence of the solution of [12]. Indeed, if $\mathcal{V}$ is a neighborhood of the compact set $\mathcal{K} = \{(t, v_t) : t \in [-d,T]\}$ then $Q$ is bounded on it and moreover $\lim_{m\to+\infty} \|Q^m - Q\|_{\mathcal{V}} = 0$. So there exists $M > 0$ such that for all $m > M$ each solution $v^m$ of:

$$\begin{cases} \frac{dv}{dt}(t) = Q^m(v_t) & t \geq 0 \\ v_0 = \phi \end{cases}$$

exists on $[-d,T]$ and $v^m \to v$ uniformly on $[-d,T]$.

### 5.1.4 The ring model of orientation tuning

In order to illustrate the previous sections, we study the ring model of orientation. This model of a hypercolumn in the primary visual cortex was first presented by Ben-Yishai [5] and then detailed by Hansel and Sompolinsky [13]. Bressloff *et al.* [6, 7] studied variants of the model by changing the form of the connectivity in the equations. First, we present the traditional model, add delays to it, and present some numerical experiments that show their influence.

We consider a network that mimicks the architecture of a cortical hypercolumn. It consists of excitatory and inhibitory neurons that respond selectively to a small oriented visual stimulus in a common receptive field. The neurons are parametrized by an angle $\theta$, ranging from $-\frac{\pi}{2}$ to $\frac{\pi}{2}$, that denotes their preferred orientation. The activity response in the network, which is the mean activity level is governed by the following equation:

$$\tau \partial_t M(\theta,t) = -M(\theta,t) + S_\mu\left( \int_{-\frac{\pi}{2}}^{\frac{\pi}{2}} J(\theta-\theta') M(\theta',t) \frac{d\theta'}{\pi} + \epsilon I(\theta-\theta_0) - \theta_{th} \right) \tag{13}$$

$\tau$ is a characteristic time assumed to be of the order of a few milliseconds. $\theta_{th}$ is the neuronal threshold. The function $J(\theta)$ represents how the interaction between neurons depends upon their preferred orientation. The input to the population of neurons encoding the orientation $\theta$ is of the form $I(\theta-\theta_0)$, where $\theta_0$ denotes the orientation for which the external input is maximal. This external current represents the lateral geniculate nucleus (LGN) input to the hypercolumn of orientations. The nonlinearity $S_\mu$ is the Heaviside function in [5, 6, 13] or a sigmoidal function in [7].

Ben-Yishai *et al.* [5] were first to propose a model of orientation tuning. They started with a network of excitatory and inhibitory spiking neurons and derived a mean field approximation that led to equation (13). The external input and the connectivity functions were set to

$$I(\theta) = 1 - \beta + \beta\cos(2\theta) \quad J(\theta) = J_0 + J_1\cos(2\theta).$$

The nonlinearity was piecewise linear, $S_\mu(x) = 0$ for $x \leq 0$, $S_\mu(x) = \mu x$ for $0 \leq x \leq \frac{1}{\mu}$ and $S_\mu(x) = 1$ for $x \geq \frac{1}{\mu}$. They had $0 \leq \beta \leq \frac{1}{2}$, $J_0 < 0$, and $J_1 > 0$. Typical values of these parameters were $\beta = 0.1, J_0 = -73, J_1 = 110, \epsilon = 1.45, \tau = 10, \theta_{th} = 1$.

Equation (13) is not of the type shown in equation (1). This is why we perform the change of variable

$$V(\theta,t) = \int_{\frac{\pi}{2}}^{\frac{\pi}{2}} J(\theta-\theta')M(\theta',t)\frac{d\theta'}{\pi} + \epsilon I(\theta-\theta_0) - \theta_{th}.$$

This leads to the following equation:

$$\tau\partial_t V(\theta,t) = -V(\theta,t) + \int_{-\frac{\pi}{2}}^{\frac{\pi}{2}} J(\theta-\theta')S_\mu\big(V(\theta',t)\big)\frac{d\theta'}{\pi} + \epsilon I(\theta-\theta_0) - \theta_{th}, \tag{14}$$

to which we add space-dependent, or rather *angle-dependent* delays:

$$\tau\partial_t V(\theta,t) = -V(\theta,t) + \int_{-\frac{\pi}{2}}^{\frac{\pi}{2}} J(\theta-\theta')S_\mu\big(V(\theta',t-\frac{|\theta-\theta'|}{c})\big)\frac{d\theta'}{\pi} + \epsilon I(\theta-\theta_0) - \theta_{th}. \tag{15}$$

The nonlinearity is the following sigmoidal function:

$$S_\mu(x) = \frac{1}{1+e^{-\mu x}} - \frac{1}{2}$$

We are now in the case of (2) with $n = q = 1$ and $\Omega = ]-\frac{\pi}{2}, \frac{\pi}{2}[$.

Roxin et al. [18] have introduced a constant delay in (13) and shown that it led to a wide variety of spatio-temporal patterns. Our model should lead to even richer sets of spatio-temporal patterns.

We did not find in the literature a biological value for the parameter $c$ for the ring model. In our numerical experiments, we set the velocity to $c = 0.2 rad.s^{-1}$.

Numerical experiments confirm that the model with delays is richer. We fix an initial condition close to zero. Figures 1(a),1(b) and 1(c) show the time evolution of the solution for $\mu = 1, 3, 10$. After a few oscillations it rapidly converges toward a stationary solution. Figure 1(d) shows the time evolution with no delays, i.e equation (14). We see that increasing the slope $\mu$ of the sigmoid seems to cause the transient oscillations to persist for longer.

## 5.2 Two populations of neurons in 1D

We consider two ($n$=2) one-dimensional ($q$=1) populations of neurons, population 1 being excitatory and population 2 being inhibitory. We have the following equations:

$$\begin{cases} \partial_t v_1(x,t) &= -\alpha_1 v_1(x,t) + \int_{-1}^{1}\big[w_{1,1}(x-y)S_1\big(v_1(y,t-\frac{|x-y|}{c_1})\big) + w_{1,2}(x-y)S_2\big(v_2(y,t-\frac{|x-y|}{c_2})\big)\big]dy \\ \partial_t v_2(x,t) &= -\alpha_2 v_2(x,t) + \int_{-1}^{1}\big[w_{2,1}(x-y)S_1\big(v_1(y,t-\frac{|x-y|}{c_1})\big) + w_{2,2}(x-y)S_2\big(v_2(y,t-\frac{|x-y|}{c_2})\big)\big]dy \end{cases} \tag{16}$$

We assume for simplicity that:

**Hypothesis 5.2.1.**

$$\alpha_1 = \alpha_2 = \alpha \quad c_1 = c_2 = c$$
$$S_1(x) = S_2(x) = S(x)$$
$$w_{i,j}(x) = \frac{a_{i,j}}{\sqrt{2\pi\sigma_{i,j}^2}} e^{-\frac{x^2}{2\sigma_{i,j}^2}} \quad a_{i,2} \le 0,\ a_{i,1} \ge 0,\ i = 1,2 \tag{17}$$

### 5.2.1 Numerical scheme

Let $E_u$ and $E_d$ be the two matrices of $\mathcal{M}_{m+1}(\mathbb{R})$ introduced in definition 5.1.1.

As usual, we use the trapezoidal rule and denote by $v_1^i(t)$ (resp. $v_2^i(t)$) the approximation $v_1(x_i,t)$ (resp. $v_2(x_i,t)$). $V_1(t)$ (resp. $V_2(t)$) is the vector of length $m+1$ with components $v_1^i(t)$ (resp. $v_2^i(t)$).

We obtain the following numerical scheme which generalizes the one of the previous section:

$$\frac{dV_1}{dt}(t) = -\alpha V_1(t) + h\sum_{k=0}^{m}\big[w_{1,1}(kh)E_k\widetilde{\mathbf{S}}\big(V_1(t-\frac{kh}{c}\big) + w_{1,2}(kh)E_k\widetilde{\mathbf{S}}\big(V_2(t-\frac{kh}{c}\big)\big]$$

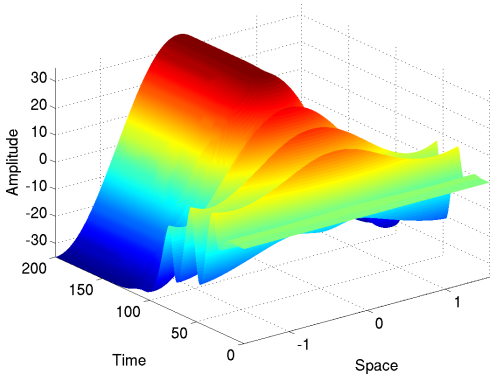


(a) Solution of (15) for $\mu = 1$, $c = 0.2$.

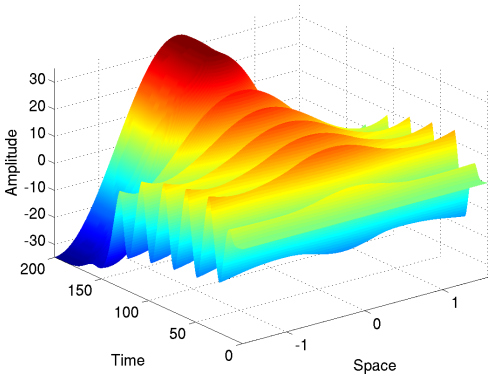


(b) Solution of (15) for $\mu = 3$, $c = 0.2$.

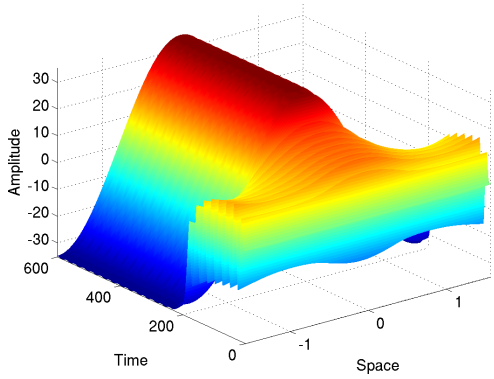


(c) Solution of (15) for $\mu = 10$, $c = 0.2$.

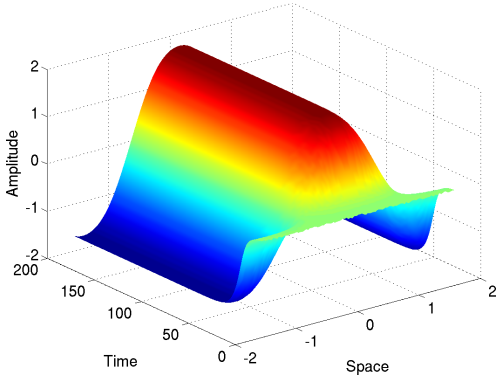


(d) Dynamic of the ring model without delay, equation (14).

Figure 1: Effect of the slope of the sigmoid on the solutions of (15).

$$\frac{dV_2}{dt}(t) = -\alpha V_2(t) + h\sum_{k=0}^{m}\big[w_{2,1}(kh)E_k\widetilde{\mathbf{S}}\big(V_1(t-\frac{kh}{c}\big) + w_{2,2}(kh)E_k\widetilde{\mathbf{S}}\big(V_2(t-\frac{kh}{c}\big)\big],$$

where $\widetilde{\mathbf{S}} : \mathbb{R}^n \to \mathbb{R}^n$ is defined by $\widetilde{\mathbf{S}}(x) = [S(x_1), \ldots, S(x_n)]^T$. We now present different numerical examples. For each example we fix the nonlinearity $S$ to be:

$$S(x) = \frac{1}{1+e^{-\mu x}} - \frac{1}{2} \tag{18}$$

### 5.2.2 Absolute stability

We begin our numerical experiments with an example of the stability result established by the method of Lyapunov functionals in section 4.2. The values of the parameters

$$\mathcal{A} = (a_{i,j}) = \begin{pmatrix} 2 & -\sqrt{2} \\ \sqrt{2} & -2 \end{pmatrix}, \quad \Sigma = (\sigma_{i,j}) = \begin{pmatrix} 1 & 0.1 \\ 0.1 & 1 \end{pmatrix} \tag{19}$$

yield $\|\tilde{W}\|_F = 0.757$. If we choose $\alpha = 1$ and $\mu = 1$ then the condition of theorem 4.2.3 is satisfied; hence the homogeneous solution $V = 0$ is uniformly asymptotically stable (absolutely stable) as we can see in figure (2) . The initial conditions are drawn randomly.

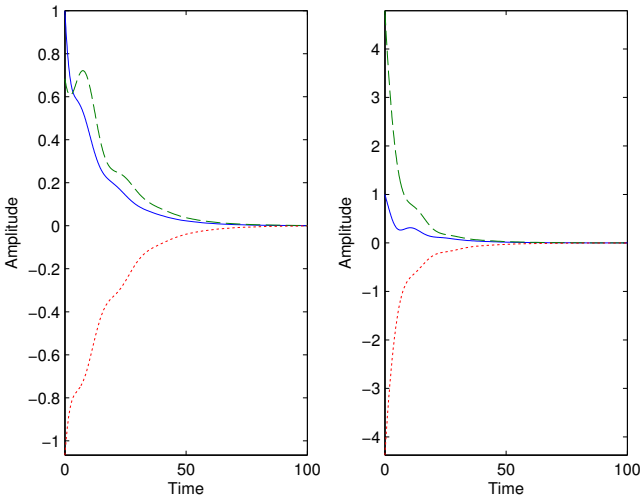


Figure 2: An illustration of the absolute stability of the fixed point at the origin: the trajectories of the state vector converge to a single trajectory, independently of the choice of the initial function. Results are shown for the neural mass of spatial coordinate: 0. Left: population 1. Right: population 2. The three curves correspond to three different initial conditions. The velocity is $c = 0.2$.

### 5.2.3 Loss of absolute stability

If we increase the value of $\|\tilde{W}\|_F$ the sufficient condition of theorem 4.2.3 will eventually not be satisfied and we may lose the absolute stability of the homogenous solution. We illustrate this remark with a numerical experiment. We choose

$$\mathcal{A} = (a_{i,j}) = \begin{pmatrix} 50.2 & -50.2 \\ 20.09 & -20.09 \end{pmatrix}, \quad \Sigma = (\sigma_{i,j}) = \begin{pmatrix} 0.1 & 0.1 \\ 1 & 1 \end{pmatrix}, \tag{20}$$

as well as $\mu = 1$, $\alpha = \frac{1}{5}$ and $c = 0.2$.
We use three different initial conditions which are all close to zero. The plots of the solutions are shown in figures (3 and 4). It is clear that we have lost the absolute stability.

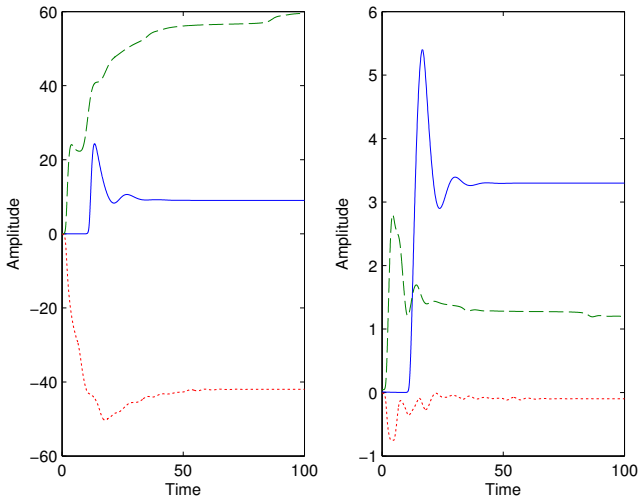


Figure 3: An illustration of the loss of absolute stability of the fixed point at the origin. Different initial conditions result in different trajectories of the state vectors. Results are shown for the neural mass of spatial coordinate: 0. Left: $V_1$. Right: $V_2$. The three curves correspond to three different initial conditions. The velocity is $c = 0.2$.

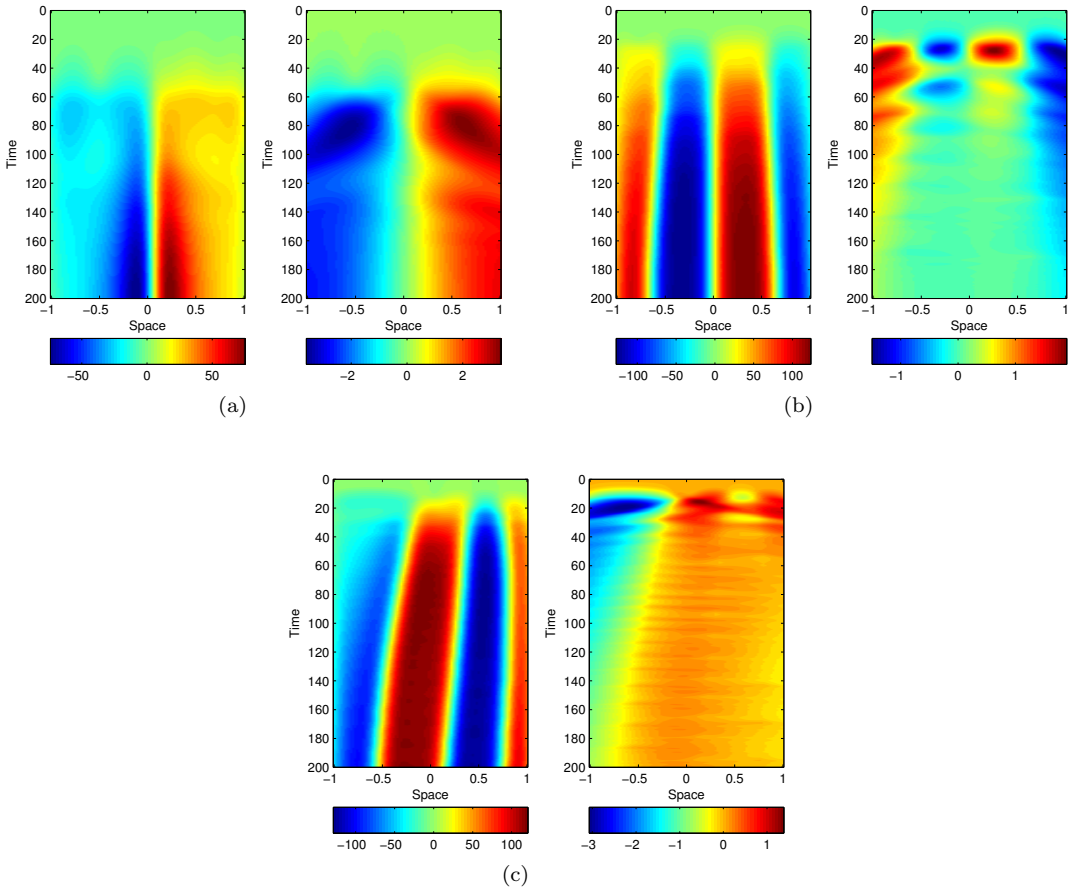


Figure 4: Another illustration of the loss of absolute stability. Space-time plot of $V_1$ (left) and $V_2$ (right) for three random initial conditions, labelled (a), (b) and (c), close to zero.

### 5.2.4 Effect of the slope $\mu$ on the solutions

We next study the effect of increasing the slope of the sigmoid. In each experiment the initial conditions are the same. We present two cases corresponding to the values of the parameters shown in (19) and (20).

In the first case, we observe that increasing the slope from $\mu = 1$ to $\mu = 3$ drastically changes the behavior of the solution. For $\mu = 1$ the system is absolutely stable and, unsurprisingly, the solution simply converges to its homogenuous state $V = 0$, as shown in figure 5(a). For $\mu = 3$ the solution oscillates in time, as shown in figure 5(b). This could be caused by a Hopf bifurcation. In order to prove this assertion we would have to perform the bifurcation analysis with respect to the parameter $\mu$ which is outside the scope of this paper. Moreover, the condition of theorem 4.2.3 is not satisfied, so we have lost the absolute stability. Indeed with $\mu = 3$, we have $\|\tilde{W}\|_F = 2.271 \geq \frac{1}{5} = \alpha$.

In the second case, we increase the slope from $\mu = 2$ to $\mu = 5$, we show the corresponding solutions in figure 6. We observe that the behaviors of the two populations have been exchanged: it appears that the plots for $\mu = 2$ and for $\mu = 5$ are related by a symmetry with respect to the plane $z = 0$, if $z$ denotes the amplitude axis. For example, when population 1 reaches its maximum in figure 6(a), it reaches its minimum in figure 6(c). As shown in figure 6(b) there exists a value $\mu_c$, which we numerically found to be close to 2.70, which separates the two kinds of activities. We are presently not able to explain this behavior.

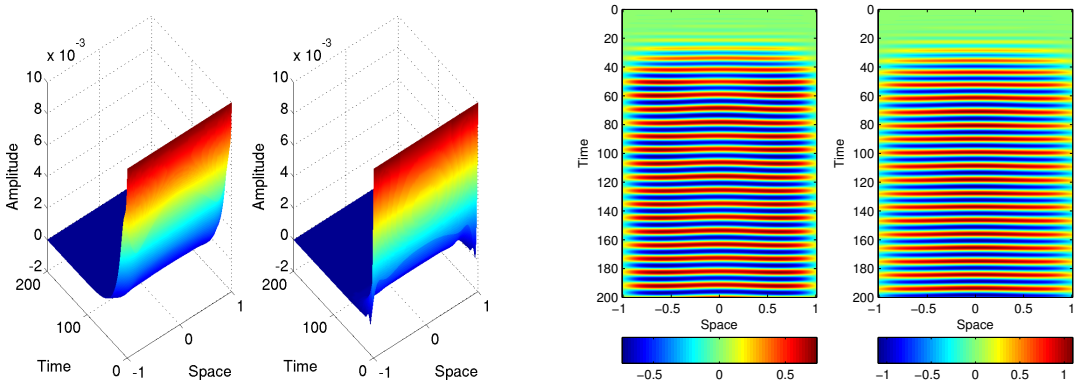


(a) Parameters are: $\mu = 1$, $c = 0.2$, and $\alpha = \frac{1}{5}$.

(b) Parameters are: $\mu = 3$, $c = 0.2$, and $\alpha = \frac{1}{5}$.

Figure 5: Effect of the slope on the solutions of equation (16) in the case of the parameters given by (19). Plots of population 1 (left) and population 2 (right) for different values of the other parameters, see text.

### 5.2.5 Effect of the delays on the solutions

In this subsection, we study the effect of the delays on the solution with the values of the parameters shown in (20). In each experiment the initial conditions are the same and we set $\mu = 2$ for the slope of the sigmoid and $\alpha = \frac{1}{5}$.

The results are presented in figure (7). For $c = 100$, the effect of the delay on the solution is reduced, relative to what is seen for smaller values of $c$. As we can expect, $c$ is a parameter of bifurcation. In figure 7(b) ($c = 10$) and 7(c) ($c = 1$) the solutions have the same behavior. Between the range of values $c = 1$ and $c = 0.1$ we observe a bifurcation. Indeed, the space-time plots of the solutions in figure 7(c), 7(d) and 7(e) show quite different behaviors.

## 5.3 One population of neurons in 2D

This section is devoted to the case of $\Omega = ]-l, l[\times]-l, l[$ with $l > 0$.

We suppose that the connectivity function $W$ is isotropic in the following sense

$$\forall r, r' \in \mathbb{R}^2 \quad W(r, r') = w(\|r - r'\|) \text{ and } d(x, y) = \frac{\|x - y\|}{c},$$

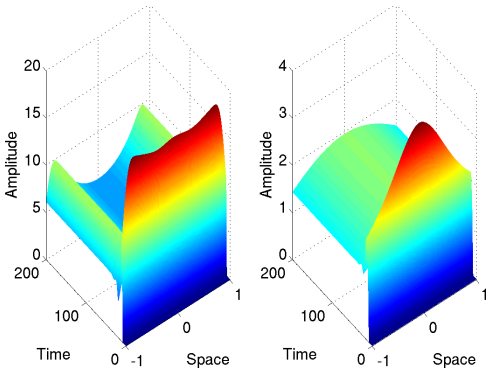


(a) Parameters are: $\mu = 2$, $c = 0.2$, $\alpha = \frac{1}{5}$.

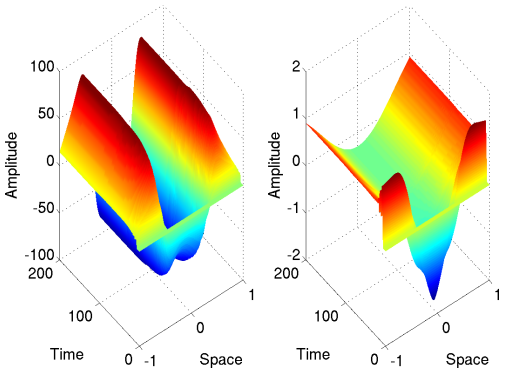


(b) Parameters are: $\mu = 2, 70$, $c = 0.2$ ,$\alpha = \frac{1}{5}$.

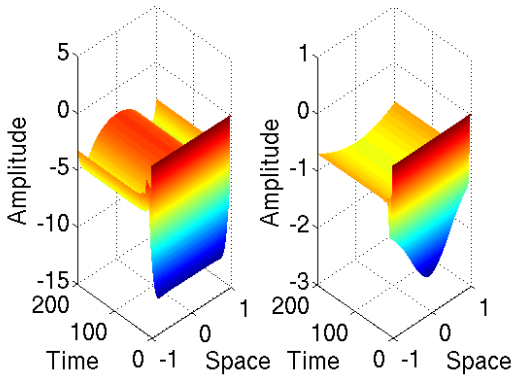


(c) Parameters are: $\mu = 5$, $c = 0.2$, $\alpha = \frac{1}{5}$.

Figure 6: Effect of the slope on the solutions of equation (16) in the case of the parameters given by (20). Plots of population 1 (left) and of population 2 (right) for different values of the other parameters, see text.

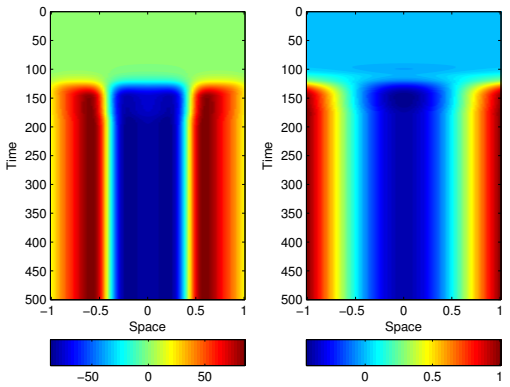


(a) $c = 100$

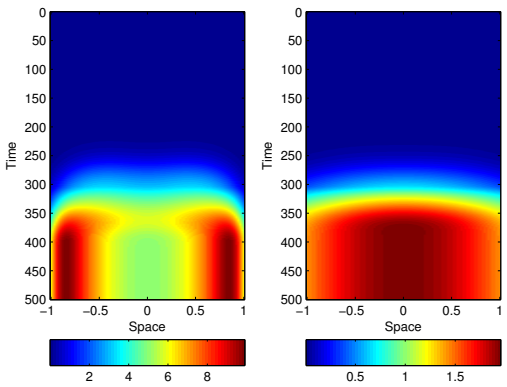


(b) $c = 10$

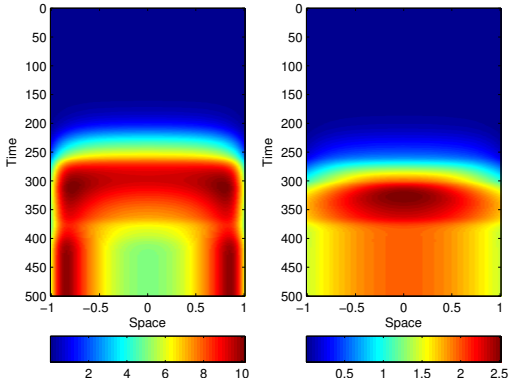


(c) $c = 1$

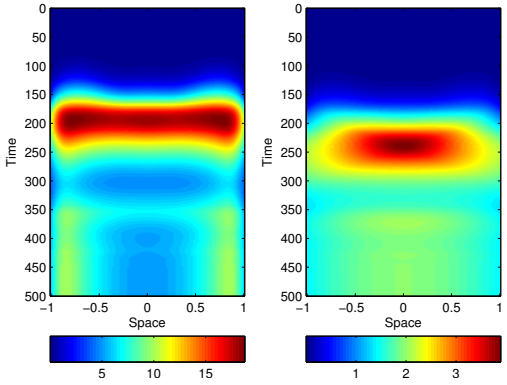


(d) $c = 0.2$

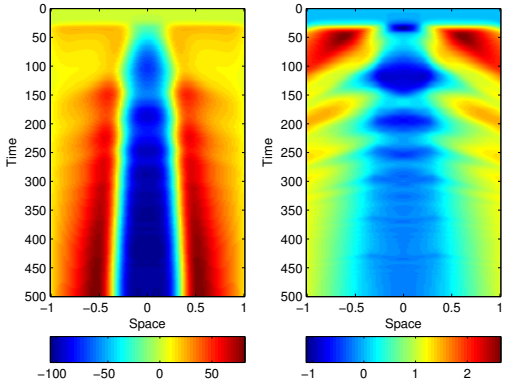


(e) $c = 0.1$

Figure 7: Effect of the delays on the solutions of equation (16). The figure shows the space-time plots of $V_1$ (left) and $V_2$ (right) for different values of the parameter $c$.

where $w : \mathbb{R}^+ \to \mathbb{R}$. We choose a connectivity function suggested by Amari in [1], commonly referred to as the "Mexican hat" connectivity. It features center excitation and surround inhibition which is an effective model for a mixed population of interacting inhibitory and excitatory neurons with typical cortical connections.

$$w(x) = \frac{1}{\sqrt{2\pi\xi_1^2}} e^{-\frac{\|x\|^2}{2\xi_1^2}} - \frac{A}{\sqrt{2\pi\xi_2^2}} e^{-\frac{\|x\|^2}{2\xi_2^2}}, \tag{21}$$

with $0 < \xi_1 \leq \xi_2$ and $0 \leq A \leq 1$.
We choose for simplicity the following norm:

$$\forall r = (x, y) \in \mathbb{R}^2 \quad \|r\|_1 = \mid x \mid + \mid y \mid$$

The choice of this particular norm instead of the usual Euclidean norm is essentially guided by their relative computational requirements: it is easier to compute $\|\cdot\|_1$ than $\|\cdot\|_2$ on a square lattice, and the number of delays that appear in the discretization scheme is very sensitive to the choice of the norm since $d(x, y) = \frac{\|x-y\|}{c}$. An easy computation shows that, if our spatial grid is $m \times m$, we obtain $2m$ different constant delays in our scheme of discretization for $\|\cdot\|_1$ as opposed to $\frac{m^2}{2}$ for $\|\cdot\|_2$. Moreover, all the norms in $\mathbb{R}^2$ are equivalent and we have the relation $\frac{\sqrt{2}}{2}\|\cdot\|_1 \leq \|\cdot\|_2 \leq \|\cdot\|_1$. This implies that for small variations of the delay, the behaviour of the solutions will not drastically change if we are not at a point of bifurcation with respect to this parameter, which is actually our case.
We plot in figure (8) the surface generated by the two different norms and compare in figure (9) a "Mexican hat" equiped with the norm 1 and the Euclidean norm.

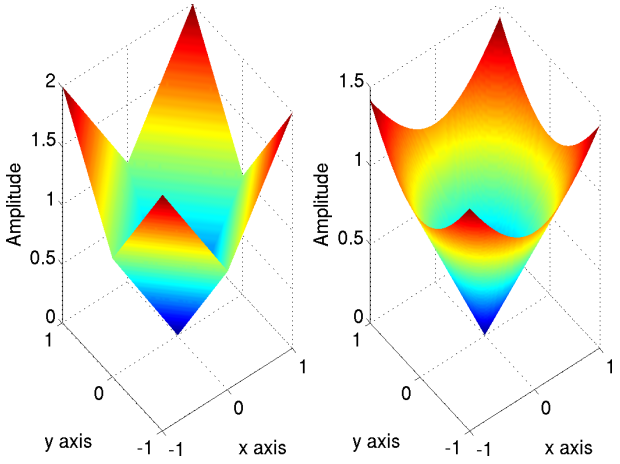


Figure 8: Left: plot of $\|\cdot\|_1$. Right: plot of $\|\cdot\|_2$.

### 5.3.1 Discretization scheme

Let $m \in \mathbb{N}^\star$ and $h = \frac{2l}{m}$. We discretize $\Omega$ with a square lattice:

$$\forall i, j = 1 \dots m+1 \quad (x_i, y_j) = \big(-l + (i-1)h, -l + (j-1)h\big),$$

and use the rectangular method for the quadrature so that for all $r = (x, y) \in \mathbb{R}^2$ we have:

$$\int_\Omega w(\|r - r'\|_1) S\big(v(r', t - \frac{\|r - r'\|_1}{c})\big) dr' \cong$$
$$h^2 \sum_{k=1}^{m+1} \sum_{l=1}^{m+1} w(\|(x, y) - (x_k, y_l)\|_1) S\big(v((x_k, y_l), t - \frac{\|(x, y) - (x_k, y_l)\|_1}{c})\big).$$

If we denote by $v_{i,j}(t)$ the approximation of $v((x_i, y_j), t)$, we obtain the following numerical scheme $\forall i, j = 1 \dots m+1$:

$$\frac{dv_{i,j}}{dt}(t) = -\alpha v_{i,j}(t) + h^2 \sum_{k=1}^{m+1} \sum_{l=1}^{m+1} w(\|(x_i, y_j) - (x_k, y_l)\|_1) S\big(v_{k,l}(t - \frac{\|(x_i, y_j) - (x_k, y_l)\|_1}{c})\big).$$

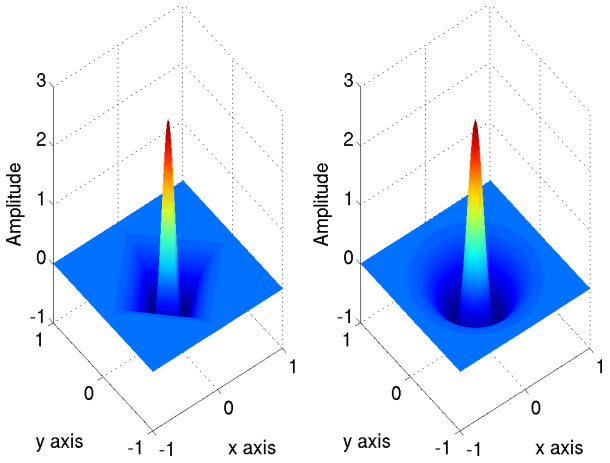


Figure 9: Plot of the "Mexican Hat" equiped with the norm 1 (left) and norm 2 (right), see text. The values are $\xi_1 = 0.1$, $\xi_2 = 0.3$ and $A = 1$.

But we have

$$\|(x_i, y_j) - (x_k, y_l)\|_1 = \|(x_i - x_k, y_j - y_l)\|_1 = \|\big((i-k)h, (j-l)h\big)\|_1 = \big(\mid i-k \mid + \mid j-l \mid\big)h,$$

and then

$$\frac{dv_{i,j}}{dt}(t) = -\alpha v_{i,j}(t) + h^2 \sum_{k=1}^{m+1}\sum_{l=1}^{m+1} w\big[\big(\mid i-k \mid + \mid j-l \mid\big)h\big] S\Big(v_{k,l}\big[t - \big(\mid i-k \mid + \mid j-l \mid\big)\frac{h}{c}\big]\Big).$$

We rewrite this system in matrix form in order to implement it in **Matlab** with the function **dde23**. We denote by $V(t)$ the matrix of the $v_{i,j}(t)$ for $i, j = 1, \ldots, m+1$, so that we have $V(t) \in \mathcal{M}_{m+1}(\mathbb{R})$. One difference with the 1D case is that the lags vector is of length $2m$: $lags = [\frac{h}{c}, \frac{2h}{c}, \ldots, \frac{2mh}{c}]$.
We rewrite the system as follows:

$$\frac{dV}{dt}(t) = -\alpha V(t) + h^2 w(0)\bar{\mathbf{S}}\big(V(t)\big) + h^2 \sum_{k=1}^{2m} w(kh)\mathbf{M}_k\Big(\bar{\mathbf{S}}\big(V(t - \frac{kh}{c})\big)\Big),$$

where $\bar{\mathbf{S}} : \mathcal{M}_{m+1}(\mathbb{R}) \to \mathcal{M}_{m+1}(\mathbb{R})$ is the function defined by:

$$\forall A \in \mathcal{M}_{m+1}(\mathbb{R}) \quad \forall i, j \quad \bar{\mathbf{S}}(A)_{i,j} = S(A_{i,j}).$$

We establish a formula for the $\mathbf{M}_k$ which are functions from $\mathcal{M}_{m+1}(\mathbb{R})$ in $\mathcal{M}_{m+1}(\mathbb{R})$. In order to do that, we have to define some matrices.

**Definition 5.3.1.** *Let $E_u$ and $E_d$ be the same two matrices of $\mathcal{M}_{m+1}(\mathbb{R})$ of definition 5.1.1. We define:*

$$\forall k = 1, \ldots, m \quad E_k = E_u^k + E_d^k$$

We now present the main result of this section.

**Theorem 5.3.1.** *We set $E_0 = \mathcal{I}_{m+1}$.*
*The numerical scheme can be written as follows:*

$$\frac{dV}{dt}(t) = -\alpha V(t) + h^2 \sum_{k=0}^{2m} w(kh) \sum_{\substack{(p,q)\in[\![0,m]\!]^2 \\ p+q=k}} E_p\Big(\bar{\boldsymbol{S}}\big(V(t - \frac{kh}{c})\big)\Big)E_q,$$

*that is:*

$$\boldsymbol{M}_k\Big(\bar{\boldsymbol{S}}\big(V(t - \frac{kh}{c})\big)\Big) = \sum_{\substack{(p,q)\in[\![0,m]\!]^2 \\ p+q=k}} E_p\Big(\bar{\boldsymbol{S}}\big(V(t - \frac{kh}{c})\big)\Big)E_q$$

*Proof.* • For all $A=(a_{i,j})_{i,j\in[\![1,m+1]\!]}\in\mathcal{M}_{m+1}(\mathbb{R})$ and $\forall p,q\in[\![1,m]\!]$ we have:

$$E_pAE_q=E_u^pAE_u^q+E_d^pAE_u^q+E_u^pAE_d^q+E_d^pAE_d^q$$

$\forall(i,j)\in[\![1,m+1]\!]^2$ the following equations hold:

$$\begin{aligned}
(E_u^pAE_u^q)_{i,j} &= \begin{cases} a_{i+p,j-q} \quad if \quad i+p\leq m+1 \quad and \quad 1\leq j-q \\ 0 \quad \text{otherwise} \end{cases}\\
(E_d^pAE_u^q)_{i,j} &= \begin{cases} a_{i-p,j-q} \quad if \quad 1\leq i-p \quad and \quad 1\leq j-q \\ 0 \quad \text{otherwise} \end{cases}\\
(E_u^pAE_d^q)_{i,j} &= \begin{cases} a_{i+p,j+q} \quad if \quad i+p\leq m+1 \quad and \quad j+q\leq m+1 \\ 0 \quad \text{otherwise} \end{cases}\\
(E_d^pAE_d^q)_{i,j} &= \begin{cases} a_{i-p,j+q} \quad if \quad 1\leq i-p \quad and \quad j+q\leq m+1 \\ 0 \quad \text{otherwise} \end{cases}
\end{aligned}$$

It follows that $\forall(i,j)\in[\![1,m+1]\!]^2$ and $\forall p,q\in[\![1,m]\!]$:

$$(E_pAE_q)_{i,j}=a_{i+p,j-q}\mathbf{1}_{\substack{1\leq j-q\\ i+p\leq m+1}}+a_{i-p,j-q}\mathbf{1}_{\substack{1\leq j-q\\ 1\leq i-p}}+a_{i+p,j+q}\mathbf{1}_{\substack{1\leq j-q\\ 1\leq i-p}}+a_{i-p,j+q}\mathbf{1}_{\substack{j+q\leq m+1\\ 1\leq i-p}}$$

- It is easy to see that we have $\forall(i,j)\in[\![1,m+1]\!]^2$ and $\forall p,q\in[\![1,m]\!]$

$$(E_0AE_q)_{i,j}=(AE_q)_{i,j}=a_{i,j-q}\mathbf{1}_{1\leq j-q}+a_{i,j+q}\mathbf{1}_{j+q\leq m+1}\quad\forall q\in[\![1,m]\!]$$

$$(E_pAE_0)_{i,j}=(E_pA)_{i,j}=a_{i+p,j}\mathbf{1}_{i+p\leq m+1}+a_{i-p,j}\mathbf{1}_{1\leq i-p}\quad\forall p\in[\![1,m]\!]$$

- $\forall(i,j)\in[\![1,m+1]\!]^2$ we obtain, through a simple change of variables, the following equality

$$\sum_{k=1}^{m+1}\sum_{l=1}^{m+1}w\big[(\mid i-k\mid+\mid j-l\mid)h\big]S\bigg(v_{k,l}\big[t-(\mid i-k\mid+\mid j-l\mid)\frac{h}{c}\big]\bigg)=$$
$$\sum_{k=0}^{2m}w(kh)\sum_{\substack{(p',q')\in[\![1,m+1]\!]^2\\ |i-p'|+|j-q'|=k}}S\big(v_{p',q'}(t-\frac{kh}{c})\big)$$

Next, $\forall k\in[\![0,2m]\!]$, we define the following matrices

$$A^k=\bar{\mathbf{S}}\big(V(t-\frac{kh}{c})\big)\quad and\quad (A^k)_{p',q'}=a^k_{p',q'}=S\big(v_{p',q'}(t-\frac{kh}{c})\big),$$

so that we have:

$$\sum_{k=0}^{2m}w(kh)\sum_{\substack{(p',q')\in[\![1,m+1]\!]^2\\ |i-p'|+|j-q'|=k}}S\big(v_{p',q'}(t-\frac{kh}{c})\big)=\sum_{k=0}^{2m}w(kh)\sum_{\substack{(p',q')\in[\![1,m+1]\!]^2\\ |i-p'|+|j-q'|=k}}a^k_{p',q'}.$$

- We next set $p=\mid i-p'\mid$ and $q=\mid j-q'\mid$, i.e.,

$$\begin{cases} p'=i\pm p\\ q'=j\pm q\end{cases}$$

This implies that $p\in[\![0,m]\!]$ and $q\in[\![0,m]\!]$.

We now fix $k \in [\![0, 2m]\!]$ to obtain

$$\sum_{\substack{(p',q')\in[\![1,m+1]\!]^2 \\ |i-p'|+|j-q'|=k}} a^k_{p',q'} =$$

$$\sum_{\substack{(p,q)\in[\![1,m]\!]^2 \\ p+q=k}} \left( a^k_{i+p,j-q}\mathbf{1}_{\substack{1\le j-q \\ i+p\le m+1}} + a^k_{i-p,j-q}\mathbf{1}_{\substack{1\le j-q \\ 1\le i-p}} + a^k_{i+p,j+q}\mathbf{1}_{\substack{1\le j-q \\ 1\le i-p}} + a^k_{i-p,j+q}\mathbf{1}_{\substack{j+q\le m+1 \\ 1\le i-p}} \right) +$$

$$a^k_{i,j-k}\mathbf{1}_{1\le j-k} + a^k_{i,j+k}\mathbf{1}_{j+q\le m+1} + a^k_{i+k,j}\mathbf{1}_{i+k\le m+1} + a^k_{i-k,j}\mathbf{1}_{1\le i-k} =$$

$$\sum_{\substack{(p,q)\in[\![1,m]\!]^2 \\ p+q=k}} (E_pA^kE_q)_{i,j} + (A^kE_k)_{i,j} + (E_kA^k)_{i,j} =$$

$$\sum_{\substack{(p,q)\in[\![0,m]\!]^2 \\ p+q=k}} (E_pA^kE_q)_{i,j} \sum_{\substack{(p,q)\in[\![0,m]\!]^2 \\ p+q=k}} \left( E_p\mathbf{S}.\big(V(t-\frac{kh}{c})\big)E_q \right)_{i,j}$$

- Finally $\forall (i,j) \in [\![1, m+1]\!]^2$:

$$\sum_{k=1}^{m+1}\sum_{l=1}^{m+1} w\big[(\,|\,i-k\,|+|\,j-l\,|\,)h\big] S\Big(v_{k,l}\big[t-(\,|\,i-k\,|+|\,j-l\,|\,)\frac{h}{c}\big]\Big) =$$

$$\sum_{k=0}^{2m} w(kh) \sum_{\substack{(p,q)\in[\![0,m]\!]^2 \\ p+q=k}} \left( E_p\bar{\mathbf{S}}\big(V(t-\frac{kh}{c})\big)E_q \right)_{i,j},$$

and:

$$\big(\frac{dV}{dt}(t)\big)_{i,j} = -\alpha(V(t))_{i,j} + \sum_{k=0}^{2m} w(kh) \sum_{\substack{(p,q)\in[\![0,m]\!]^2 \\ p+q=k}} \left( E_p\bar{\mathbf{S}}\big(V(t-\frac{kh}{c})\big)E_q \right)_{i,j}.$$

This concludes the proof of the theorem.

□

### 5.3.2 Remark

We have already discussed the link between the quadrature rule used in the discretization scheme and the final error of convergence in 5.1.2. The remark remains relevant in the 2D case where our scheme is based on the rectangular rule. The error of the rule is well-known in the 1D case: if $f$ is $\mathcal{C}^1$ on an interval $[a, b]$ the error is $\frac{(b-a)^2}{2m^2} f'(\xi)$ for some $\xi \in [a, b]$ where $m$ is the number of subintervals used. This error still holds in the case of a function $f$ which is $\mathcal{C}^2$ on a rectangular domain $[a, b] \times [c, d]$. If we denote by $E_f$ this error, then $|E_f| \le \frac{(b-a)^2(d-c)^2}{4mn}\|f\|_{\mathcal{C}^2}$ where $m$ and $n$ are the number of subintervals used and $\|f\|_{\mathcal{C}^2} = \sum_{|\alpha|\le 2} \sup_{[a,b]\times[c,d]} |\partial^\alpha f|$ where, as usual, $\alpha$ is a multi-index. Then if we want to control the error, we have to impose that the solution is, at least, $\mathcal{C}^2$ in space.
We can also establish a proof of the convergence of the numerical scheme which is exactly the same as in 5.1.3.

### 5.3.3 Numerical experiments

We use the "Mexican hat" connectivity (21) and the usual sigmoidal nonlinearity.

**Purely excitatory connectivity** In these experiments we choose $\xi_1 = 0.3$ and $A = 0$ in (21). We fix $l = 1$ for $\Omega$ and use $m = 30$ for the discretization in space.

For $\mu = 1$ the system is absolutely stable and, unsurprisingly, the solution simply converges to its homogeneous state $V = 0$, as shown in figure 10(a). Increasing the slope from $\mu = 1$ to $\mu = 10$ changes the behavior of the solution. Indeed, in figure 10(b), almost all the network is excited, in agreement with the choice of a purely excitatory connectivity.

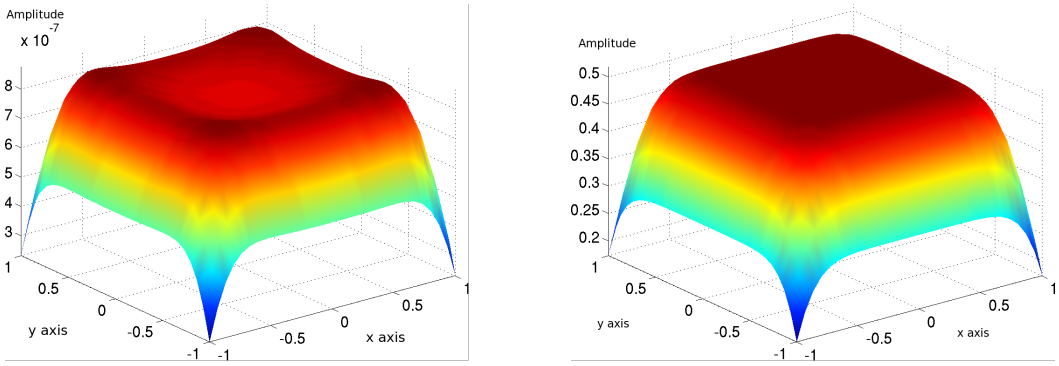


(a) $\mu = 1$ (b) $\mu = 10$

Figure 10: Plots of the solution of equation (2) at $T = 700$ for $n = 1$ and $q = 2$, for the values $\xi_1 = 0.3$ and $A = 0$ in (21) and for different parameters of the slope of the sigmoid, see text. Note the difference in vertical scales of a factor $10^{-7}$.

**Mexican hat connectivity** In this subsection, we present several experiments for two different Mexican hat connectivities. In both cases we increase the slope of the sigmoid from $\mu = 25$ to $\mu = 45$.

First we choose $\xi_1 = 0.1$, $\xi_2 = 0.2$ and $A = 1$ in (21). The results are shown in figure 11 at the same time $T = 700$ for the three values 25, 35, and 45 of the slope $\mu$ of the sigmoid. For each slope value the solutions are displayed as a perspective view (left in the figure) and as an image (right in the figure). We observe the emergence of periodic square patterns that seem to indicate that the solution is converging toward a simple biperiodic function. This impression is confirmed by figure 12 where we plot the guessed function $x \mapsto \cos(13\|x\|_1)$ over $[-l, l] \times [-l, l]$ which is essentially the same as the solution obtained for $\mu = 45$ in 11(f). We note that the norm $\|\cdot\|_1$ strongly influences the solutions.

Second we choose the connectivity $\xi_1 = 0.2$, $\xi_2 = 0.3$ and $A = 1$ in (21) in order to discover new patterns of activity. The corresponding solutions at $T = 700$ are shown in figure 13 for the values 25 and 45 of the slope $\mu$. Just as in the previous case we observe the emergence of periodic square patterns that seem to indicate that the solution is converging toward a simple biperiodic pattern. This impression is confirmed by figure 14 where we plot the guessed function $(x, y) \mapsto \cos(7x)\cos(7y)$ over $[-l, l] \times [-l, l]$ which is essentially the same as the solution obtained for $\mu = 45$ in 13(d).

# 6 Conclusion

We have studied the existence, uniqueness, and asymptotic stability of a solution of nonlinear delay integro-differential equations that describe the spatio-temporal activity of sets of neural masses. We have also developed approximation and numerical schemes.

Using methods of functional analysis, we have found sufficient conditions for the existence and uniqueness of these solutions for general inputs. We have developed a Lyapunov functional which provides sufficient conditions for the solutions to be asymptotically stable. These conditions involve the connectivity functions and the slopes of the sigmoids as well as the time constant used to describe the time variation of the postsynaptic potentials.

We have developed numerical schemes for one- and two-dimensional models. These numerical schemes consist of approximating the integral part of the righthand side of our equation with the trapezoidal rule in 1D and the rectangular rule in 2D to reduce the integro-differential equations to a finite set of delayed differential equations and in relying on the **dde23 Matlab** routine to solve these equations. The error between the continuous and the discrete equations has been bounded, see section 5.1.2 in 1D, and section 5.3.2 in 2D. We have sketched proofs of the convergence of our approximation and numerical schemes. They have allowed us to explore a large number of numerical examples.

To our knowledge, this is the first time that such a complete analysis of the problem of the existence and uniqueness of a solution of these equations has been obtained. It is also the first time that a Lyapunov functional has been introduced to contribute to the analysis of the asymptotic stability of these solutions.

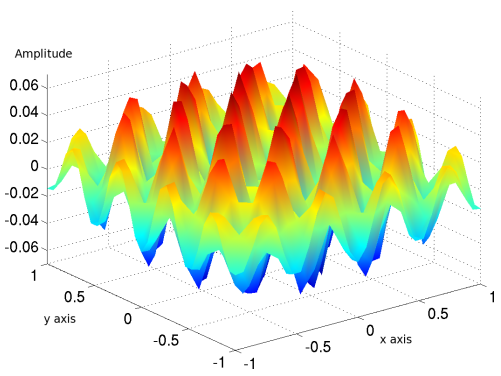


(a) $\mu = 25$

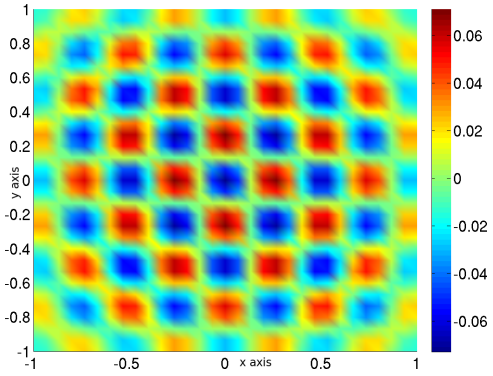


(b) $\mu = 25$

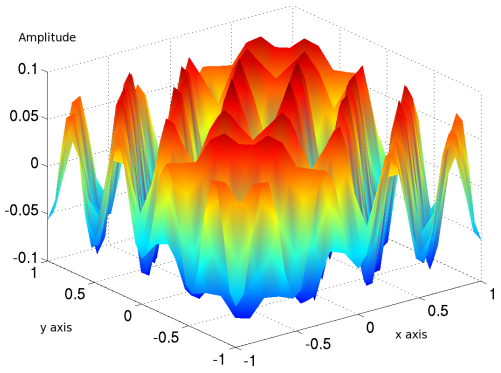


(c) $\mu = 35$

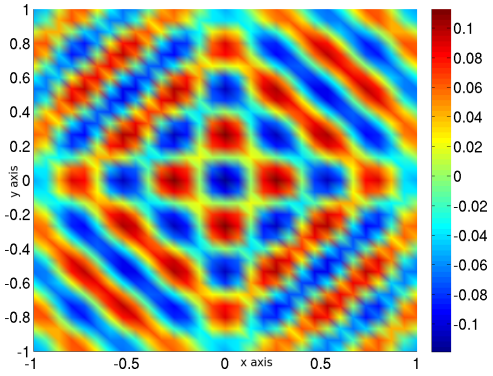


(d) $\mu = 35$

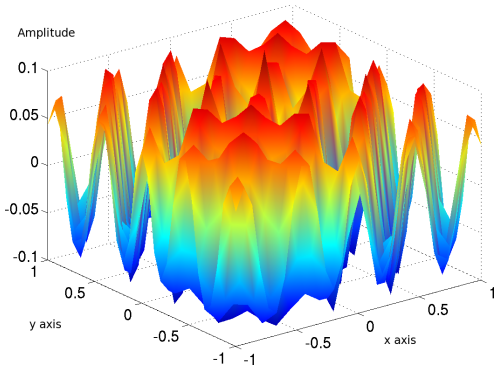


(e) $\mu = 45$

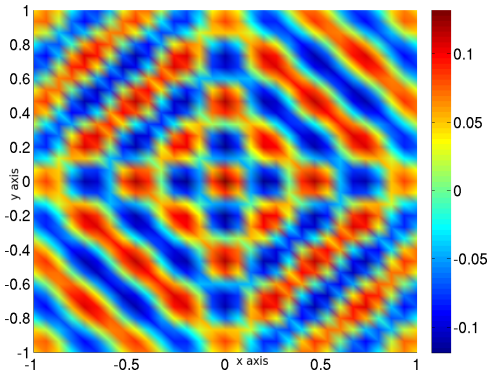


(f) $\mu = 45$

Figure 11: Plots of the solution of equation (2) at $T = 700$ for $n = 1$, $q = 2$, for the values $\xi_1 = 0.1$, $\xi_2 = 0.2$ and $A = 1$ in (21) and for increasing values of the slope $\mu$ of the sigmoid, see text.

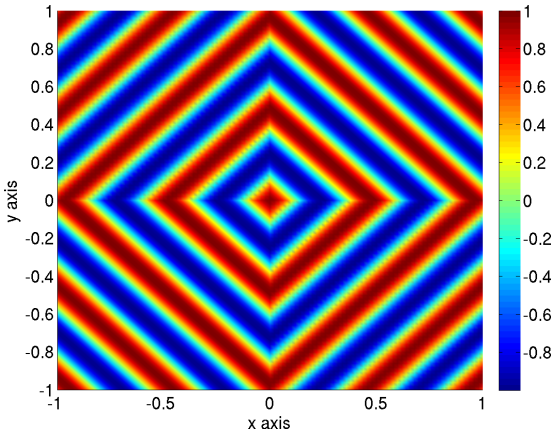


Figure 12: Plot of the function $(x, y) \mapsto \cos(13\|(x, y)\|_1)$. Note the similarity with figure 11(f)

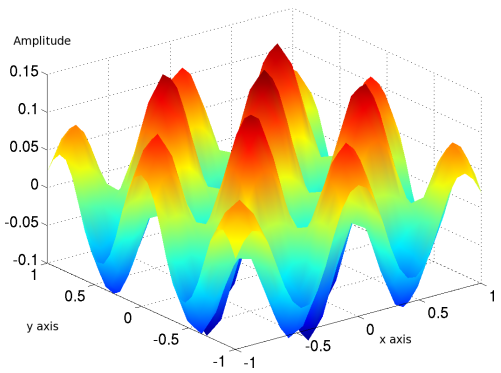


(a) $\mu = 25$

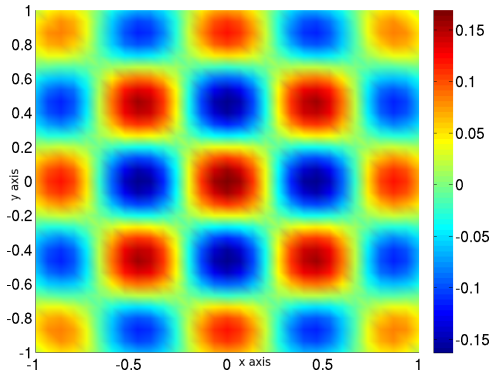


(b) $\mu = 25$

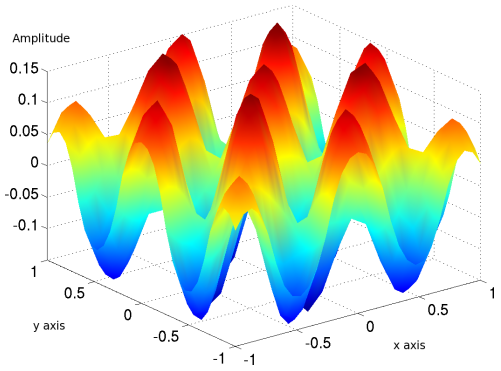


(c) $\mu = 45$

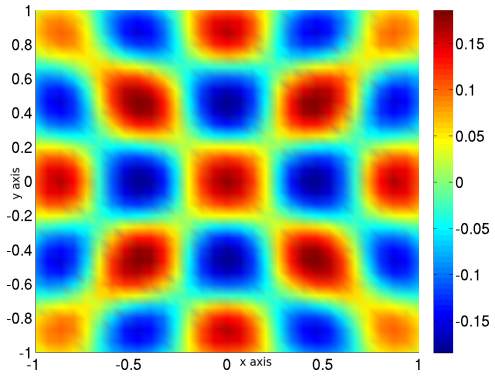


(d) $\mu = 45$

Figure 13: Plots of the solution of equation (2) at $T = 700$ for $n = 1$, $q = 2$, for the values $\xi_1 = 0.2$, $\xi_2 = 0.3$ and $A = 1$ in (21) and for increasing values of the slope $\mu$ of the sigmoid, see text.

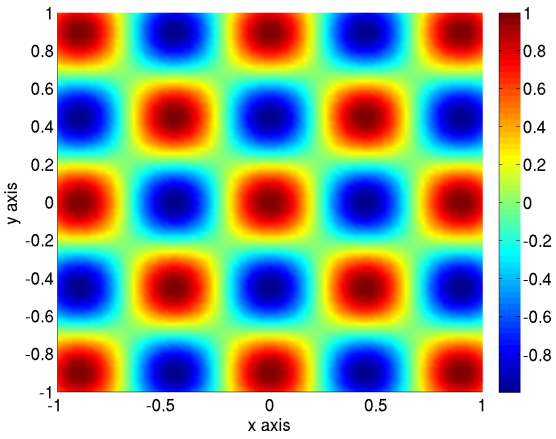


Figure 14: Plot of the function $(x, y) \mapsto \cos(7x)\cos(7y)$.

We hope that our numerical schemes and experiments will lead to new and exciting investigations such as a thorough study of the bifurcations of the solutions of our equations with respect to such parameters as the slope of the sigmoid and the delays.

**Acknowledgments**
This work was partially funded by the ERC advanced grant NerVi number 227747.

# References

[1] S.-I. Amari. Dynamics of pattern formation in lateral-inhibition type neural fields. *Biological Cybernetics*, 27(2):77–87, jun 1977.

[2] Fatihcan M. Atay and Axel Hutt. Stability and bifurcations in neural fields with finite propagation speed and general connectivity. *SIAM Journal on Applied Mathematics*, 65(2):644–666, 2005.

[3] Fatihcan M. Atay and Axel Hutt. Neural fields with distributed transmission speeds and long-range feedback delays. *SIAM Journal of Applied Dynamical Systems*, 5(4):670–698, 2006.

[4] A. Bellen and M. Zennaro. *Numerical Methods for Delay Differential Equations*. Oxford Science Publications, 2005.

[5] R. Ben-Yishai, RL Bar-Or, and H. Sompolinsky. Theory of orientation tuning in visual cortex. *Proceedings of the National Academy of Sciences*, 92(9):3844–3848, 1995.

[6] P.C. Bressloff, N.W. Bressloff, and J.D. Cowan. Dynamical mechanism for sharp orientation tuning in an integrate-and-fire model of a cortical hypercolumn. *Neural computation*, 12(11):2473–2511, 2000.

[7] P.C. Bressloff, J.D. Cowan, M. Golubitsky, P.J. Thomas, and M.C. Wiener. Geometric visual hallucinations, Euclidean symmetry and the functional architecture of striate cortex. *Phil. Trans. R. Soc. Lond. B*, 306(1407):299–330, mar 2001.

[8] S. Coombes and C. Laing. Delays in activity based neural networks. *Philosophical Transactions of the Royal Society A.*, 367:1117–1129, 2009.

[9] S. Coombes, N.A Venkov, L. Shiau, I. Bojak, D.T.J. Liley, and C.R. Laing. Modeling electrocortical activity through local approximations of integral neural field equations. *Physical Review E*, 76(5):51901, 2007.

[10] J.E Desmedt and G. Cheron. Central somatosensory conduction in man: neural generators and interpeak latencies of the far-field components recorded from neck and right or left scalp and earlobe. *Journal of Electroencephalography and Clinical Neurophysiology*, 5:382–403, 1980.

[11] J.K. Hale. A stability theorem for functional-differential equations. *Proceedings of the National Academy of Sciences*, 50:942–946, 1963.

[12] J.K. Hale and S.M.V. Lunel. *Introduction to functional differential equations*. Springer Verlag, 1993.

[13] D. Hansel and H. Sompolinsky. Modeling feature selectivity in local cortical circuits. *Methods of neuronal modeling*, pages 499–567, 1997.

[14] A. Hutt. Local excitation-lateral inhibition interaction yields oscillatory instabilities in nonlocally interacting systems involving finite propagation delays. *Physics Letters A*, 372:541–546, 2008.

[15] A. Hutt and F.M. Atay. Effects of distributed transmission speeds on propagating activity in neural populations. *Physical Review E*, 73(021906):1–5, 2006.

[16] A. Hutt and F.M. Atay. Spontaneous and evoked activity in extended neural populations with gamma-distributed spatial interactions and transmission delay. *Chaos, Solitons and Fractals*, 32:547–560, 2007.

[17] A. Hutt, M. Bestehorn, and T. Wennekers. Pattern formation in intracortical neuronal fields. *Network: Computation in Neural Systems*, 14:351–368, 2003.

[18] A. Roxin, N. Brunel, and D. Hansel. Role of Delays in Shaping Spatiotemporal Dynamics of Neuronal Activity in Large Networks. *Physical Review Letters*, 94(23):238103, 2005.

[19] L.F. Shampine and S. Thompson. Solving ddes in matlab. *Applied Numerical Mathematics*, 37:441–458, 2001.

[20] G. Shepherd. *Neurobiology*. Oxford University Press, New-York, 1994.

[21] N.A. Venkov. *Dynamics of Neural Field Models*. PhD thesis, University of Nottingham, 2008. URL: http://www.maths.nottingham.ac.uk/personal/pmxnav/nikola venkov 09 - neural fields - phd thesis.pdf.

[22] N.A. Venkov, S. Coombes, and P.C. Matthews. Dynamic instabilities in scalar neural field equations with space-dependent delays. *Physica D: Nonlinear Phenomena*, 232:1–15, 2007.

[23] H.R. Wilson and J.D. Cowan. Excitatory and inhibitory interactions in localized populations of model neurons. *Biophys. J.*, 12:1–24, 1972.

[24] H.R. Wilson and J.D. Cowan. A mathematical theory of the functional dynamics of cortical and thalamic nervous tissue. *Biological Cybernetics*, 13(2):55–80, sep 1973.

[25] J. Wu. *Theory and applications of partial functional differential equations*. Springer, 1996.